Norwegian Meteorological Institute
met.no
met.no report

no. 12/2005
Climate

Empirical-statistical downscaling of distribution functions for daily precipitation

RegClim results

Rasmus E. Benestad, Christine Achberger, & Elodie Fernandez

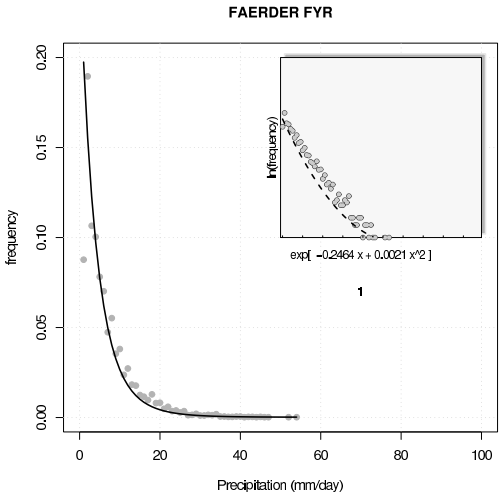

Log-linear distribution of 24-hr precipitation.

Norwegian
Meteorological Institute
met.no

report

Title	Date
Empirical-statistical downscaling of distribution functions for daily precipitation	19th September 2005
Section Climate	**Report no.** 12/2005
Author Benestad, Achberger & Fernandez	**Classification** ● Free ○ Restricted
	ISSN 1503-8025
	e-ISSN 1503-8025
Client(s)	**Client's reference**

Abstract A relatively new approach based on predictions of the parameters of a variable's distribution functions is a promising method for downscaling daily precipitation. Here, two different approaches are investigated, one assuming that the precipitation follows a Gamma distribution and one assuming a simpler exponential distribution law requiring one parameter only. The scale and shape parameters for the Gamma distribution and the slope parameter for the exponential function are tested for dependencies against large-scale climatic conditions. The number of rainy days and shape parameters can be associated with the large-scale circulation, but the relationship between the scale and the atmospheric flow is weak at best. The slope parameter for the exponential distribution exhibits a strong dependency to local mean temperature, mean precipitation and altitude. The dependency between these parameters and climate variables is utilised in a projection of the frequency distribution for 24hr precipitation for an SRES-A1b-based climate-change scenario for 2070.

Keywords
Empirical downscaling, precipitation, distribution, climate change.

Disciplinary signature	Responsible signature
Rasmus Benestad	Eirik Førland

Postal address
P.O Box 43 Blindern
N-0313 OSLO
Norway

Office
Niels Henrik Abels vei 40

Telephone
+47 2296 3000

Telefax
+47 2296 3050

e-mail: met.inst@met.no
Internet: met.no

Bank account
7694 05 00601

Swift code
DNBANOKK

Contents

1 Introduction

Perhaps the most important effect of a climate change is a shift in the local precipitation statistics. An increase in the frequency or amount of extreme rainfall can lead to flooding (*Schmidli & Frei*, 2005), and an increase in the length of dry spells can lead to droughts. Both effects have severe consequences for the local communities and ecosystems.

Empirical downscaling of daily precipitation is notoriously difficult (*Schoof & Pryor*, 2001). However, there has been a number of downscaling studies for 24hr precipitation, based on regression type models as well as non-linear models. *Abaurrea & Asín* (2005) used a regression based model for daily rainfall at a Spanish site, using predictors representing one grid point. One problem with using one grid point may be the limitations due to GCMs' skillful spatial scales (*von Storch* et al., 1993; *Grotch & MacCracken*, 1991). Another problem is that daily precipitation does not usually follow a Gaussian distribution (*Wilks*, 1995), i.e. its probability distribution function is not 'bell-shaped'. Ordinary regression analysis assumes that the data and the errors have pdfs that are Gaussian in order to obtain unbiased results. We will henceforth use the standard abbreviation 'pdf' in the meaning of 'probability distribution function' (or statistically modelled frequency distribution).

A simple non-linear approach known as 'weather analogs' can be employed to circumvent the problem of being non-Gaussian distributed. The 'analog method' consists of searching for a situation in the past that resembles a given atmospheric state the most, and use observations for that day in order to make a prediction (*van den Dool*, 1995; *Zorita & von Storch*, 1999; *Dehn*, 1999; *Fernandez & Saenz*, 2003; *Imbert*, 2003). Although the analog method appears to be a robust method that yields realistic variance (*Fernandez*, 2005; *Imbert*, 2003), *Imbert & Benestad* (2005) argued that it cannot produce new record-breaking values as the predicted range is determined by the historical sample. A temporal disaggregation scheme utilised by *Salathé* (2005) based on monthly analogs in order to prescribe daily precipitation and temperature also suffers from the same shortcoming. Even for a variable that is independent and identically distributed (iid) new record-breaking events are expected over time as the as the number of realisations grows (*Benestad*, 2004b, 2003). Although the occurrence of new record-breaking values is expected to diminish for iid data as the length observational series grows, a sign of non-iid behaviour can indicate that the upper tail of a pdf is being stretched if a dependency between the different values can be ruled out, and that the analog model is inappropriate.

The analog may not be capable of predicting changes to the tails of a pdf characterising extremes if the tails of the pdf undergo changes. However, if the type of pdf is known for a given variable, then it may be possible to account for the changes in its tails if the shape of the distribution (the fitted parameters) is related to the large-scale circulation. *Feuerstein* et al. (2005) observed what they regarded a 'universal feature' for tornadoes, concluding that the Weibull parameters describing the intensity had shape and scale that are correlated. If there exist other universal features, such as a systematic relationship between the shape of the pdf for 24hr precipitation and other characteristics such as the large-scale atmospheric flow or the local mean climate, then this information may be utilised in the projections for climate-change studies. Empirical downscaling has been applied to distribution functions with some degree of success (*Hayhoe* et al., 2004; *Pryor* et al., submitted).

This report gives an overview over different approaches for relating the best-fit parameters for two different types of pdf: the Gamma distribution and the exponential law. The data are presented

in the next section followed by the discussion on the methods. Then the results are given for both the approach based on the Gamma distribution as well as that of the exponential law. The analysis is then extrapolated to make future projections of the pdf for 24hr precipitation for a selection of locations, followed by a discussion, conclusion and appendices.

2 Data & Methods

2.1 Data

2.1.1 Data for calibration and evaluation of statistical models

Gridded sea level pressure, temperature and precipitation used as predictors in the downscaling analysis were taken from the ECMWF ERA40 reanalysis (*Simmons & Gibson*, 2000), while the daily precipitation and temperature data were taken from the Data archive of the Norwegian Meteorological Institute and from ECSN (*Klein Tank* et al., 2002). In addition, for the spatial analysis (Section 3.2.1) even daily precipitation from a number of Swedish stations provided by the Swedish Meteorological and Hydrological Institute (SMHI) for the period 1961-200 were used.

2.1.2 Data for making future scenarios

Scenarios for local climate change were obtained from the analysis by *Benestad* (2005) and consisted of a multi-model ensemble Bayesian analysis of 12 different global climate models (GCMs), but 21 and 23 different integrations for precipitation and temperature respectively (see Table 1). The scenarios derived by *Benestad* (2005) were for annual mean values, which were also utilised for this study extrapolating future pdfs for the all-year rainfall. One important caveat is that the trend in precipitation may differ from season to season, and the extrapolations presented here should therefore be regarded as tentative at this stage. The GCMs results were based on the IPCC SRES A1b emission scenario. The best estimate of the temperature- or precipitation-change at a given location was based on a quality weighted mean linear trend from individually downscaled results. Further details about the quality testing is given in *Benestad* (2005).

2.2 Methods

The calibration interval for the downscaling (including the analog) model was 1957–1999. The downscaling of the precipitation was done through a number of approaches:

(i) Downscaling the Gamma parameters α and β for a given season (a 'season' is defined here as a 3-month interval: December–February, March–May, June–July, or September–October).

(ii) Downscaling the seasonal mean of precipitation for rainy days and the standard deviation of corresponding precipitation and subsequently estimate Gamma parameters.

(iii) Downscaling the transforms of Gamma parameters $\sqrt{\alpha}$ and $1/\beta$ and subsequently apply the inverse transform.

GCM Temperature	Run	m_{GCM} Precipitation	GCM	Run	m_{GCM}
CNRM-CM3	1	1	CNRM-CM3	1	1
GFDL-CM2.0	1	1	GFDL-CM2.0	1	1
GFDL-CM2.1	1	1			
GISS-AOM	1,2	2	GISS-AOM	1,2	2
GISS-EH	1–3	3	GISS-EH	1–3	3
GISS-ER	4	1	GISS-ER	4	1
INM-CM3.0	1	1	INM-CM3.0	1	1
IPSL-CM4	1	1	IPSL-CM4	1	1
ECHAM5/MPI-OM	1–3	3	ECHAM5/MPI-OM	1,3	2
MRI-CGCM2.3.2	1–5	5	MRI-CGCM2.3.2	1–5	5
CCSM3	1,2	2	CCSM3	1,2	2
PCM	2	1	PCM	2	1
UKMO-HadCM3	1	1	UKMO-HadCM3	1	1
		23			21

Table 1: Number of different GCM runs used in the multi-model ensemble.

(iv) using an analog model for downscaling daily values.

(v) using a linear (multiple regression) model for downscaling daily values.

(vi) using local observed or downscaled mean temperature and mean precipitation to make a prediction for the slope m for the exponential e^{c+mx}(and the coefficients for the higher order terms: eg $e^{c+m_1x+m_2x^2}$).

(vii) using downscaled mean temperature and mean precipitation to make a prediction for the Gamma parameters.

2.2.1 (i)–(iii):The Gamma distribution

The objective of this study was to reproduce the distribution of the 24-hour precipitation amounts using a statistical distribution model. One common approach has been to use a Gamma model to represent the observed distribution, as this function can have a shape that follows the empirical shape given two tuned parameters. The pdf for the Gamma distribution, $f(x)$, is described by following expression:

$$f(x) = \left(\frac{x}{\beta}\right)^{\alpha-1} \frac{\exp[-x/\beta]}{\beta\Gamma(\alpha)}, x, \alpha, \beta > 0. \quad (1)$$

where α is the 'shape', β the 'scale' parameter, and $\Gamma(\alpha) = \int_0^\infty t^{\alpha-1}e^{-t}dt$. There are different ways of estimating the two paramterers, of which the moment estimator (*Wilks*, 1995, p. 89) is the simplest:

$$\hat{\alpha} = \frac{(\overline{x_R})^2}{s^2}, \tag{2}$$

$$\hat{\beta} = \frac{s^2}{\overline{x_R}}, \tag{3}$$

where $\overline{x_R}$ is the mean value for the rainy days (here, day with rainfall greater than 1mm) only and s corresponding standard deviation. These should not be confused with the more traditional 'seasonal means' ($\overline{x}$) which are estimated for the entire season (both dry and rainy days). *Wilks* (1995) states that the moment estimators are "inefficient" and lead to erratic estimates, and recommends using the so-called maximum likelihood estimators:

$$\hat{\alpha} = \frac{1 + \sqrt{1 + 4D/3}}{4D}, \tag{4}$$

$$\hat{\beta} = \overline{x_R}/\hat{\alpha}, \tag{5}$$

$$D = \ln(\overline{x_R}) - 1/n \sum_{i=1}^{n} \ln(x_i). \tag{6}$$

The central question here is whether the Gamma parameters for a given location are systematically influenced by either the large-scale conditions or the local geography in such a way that they can be predicted given this information. Such predictions are in essence the same as 'downscaling'.

The transform-approach (iii) was motivated by the fact that

$$\overline{x_R} = s\sqrt{\alpha}, \overline{x_R} = s^2/\beta, \tag{7}$$

and that a large fraction of the monthly mean precipitation ($\overline{x}$) can be predicted by downscaling models (*Benestad* et al., submitted). Seasonal values of SLP, T(2m) and precipitation were used for downscaling (also using a linear multiple regression model of `clim.pact`) *seasonal values for the Gamma parameters*.

2.2.2 (iv) The analog model

The analog model is described in *Fernandez* (2005); *Imbert & Benestad* (2005); *Imbert* (2003) and the linear downscaling model (`clim.pact`) in *Benestad* (2004a) and references therein. Daily SLP from ERA40 were used as predictors for both the analog and the linear model for local *daily precipitation*.

2.2.3 (v) The linear model

For the reason of comparisons, one downscaling exercise was based on linear multiple-regression using the `clim.pact` in a standard mode. More documentation about the model is found in *Benestad* (2004a); *Imbert & Benestad* (2005).

2.2.4 (vi) The exponential law

An exponential distribution function was fitted to the 24-hour precipitation by regressing linear as well as 2–3 order polynomials to the linear-log relationships seen in Figure 1. In many cases, the empirical linear-log distribution was close to linear, but some places with warm climates had a tendency of many dry days. However, when it rains in these locations, heavy rainfall is relatively frequent. The heavy rainfall events gave rise to thick upper tails in the distribution and the need for using higher-order polynomial models for a better description of the distribution. In some places characterised by a wet climate, such as Glomfjord, there was also a high proportion of days with heavy rainfall and hence fat upper tails.

The best-fit of the exponential models was obtained applying a linear regression between the logarithm of the frequency, as a function of the amount of precipitation, and a linear or 2nd–3rd order polynomials. A weighting was applied to for regression fit for the linear model $f(x) = e^{-mx}$ ($w_i = \sqrt{n_i}/\sum_k \sqrt{n_k}$), but not for the more complex models utilising 2nd and 3rd order polynomials since these were introduced to capture the thicker tails for the more rare events of heavy precipitation.

Regression analysis was employed in the search for systematic dependencies of the fitted functions to large-scale state of the atmosphere or local climate characteristics. The depending variables were mean temperature, mean precipitation amount, altitude, distance from the coast, number of rainy days and the R^2-statistic indicating the goodness of linear fit to the log-linear distribution function. Longitude and latitude were excluded since latitude correlated strongly with the mean temperature and the stepwise screening would sometimes select latitude rather than mean temperature. We wanted to keep the explicit temperature dependency which is utilised in the 'downscaling' for a future climate. The zonal distance is not linearly related with longitude but is latitude dependent.

Europe can be represented by different climate zones similar to Köppen's macro-climate classifications (*Tveito & Førland*, 1999). It is plausible that a climate change will entail an expected migration of these climate zones, hence providing a justification for using extrapolations based on spatial variations. However, the concept of 'migrating climate zones' is probably more true for temperature than for precipitation. Furthermore, such extrapolations may not be valid for all locations as some climate zones are strongly influenced by different mechanisms, such as the local physiography.

3 Results

3.1 Fit to statistical models for distribution

Figure 1 shows a number of linear-log plots for the distribution of 24-hour precipitation amounts for 49 different European locations. The grey dots represent the empirical results (histogram with log y-axis) and the dashed black lines show the distribution model fit. The different distribution models include 3 exponential models as well as the Gamma model (using moments estimators). It is evident from this figure that the character of the distribution (e.g. the slope m) varies from place to place. The interesting question here is whether there is a systematic dependency between the slope m and the large-scale flow regime or dominant characteristics of the local climate.

Similar near-linear behaviour can be seen in similar log-linear distribution of tornadoes of category

F1 and greater (*Feuerstein* et al., 2005, Fig. 2a). *Feddersen & Andersen* (2005) have used exponential distribution to approximate the pdf for 24-hour precipitation in Denmark.

3.2 Gamma distribution

Figure 2 shows a comparison between the different estimators for daily precipitation for the different seasons in Oslo. These results suggest that both the scale and the shape of the distribution function varies over time. In order to explore possible relationships between these parameters and the large-scale conditions, sets of correlation analyses and downscaling exercises were carried out.

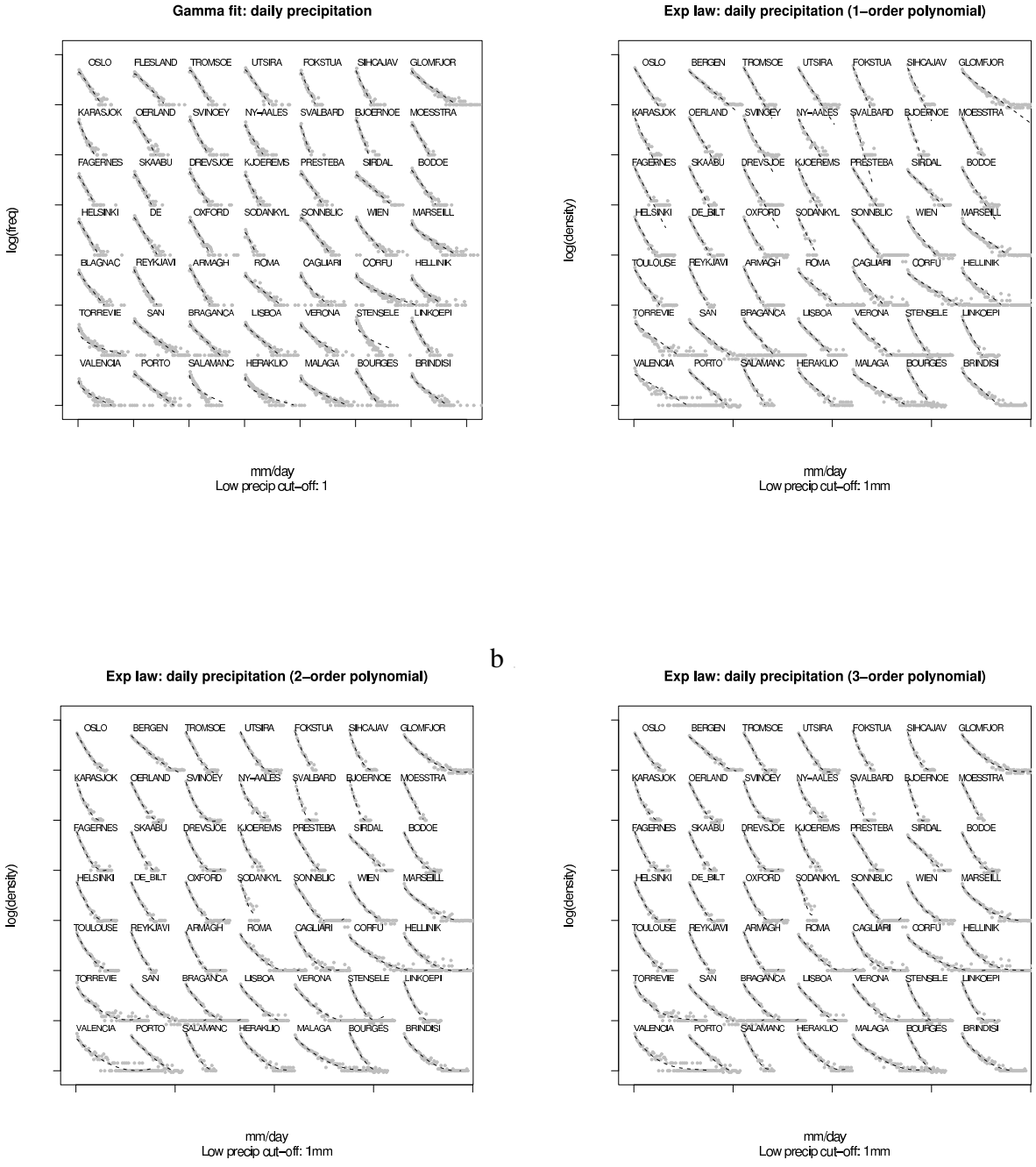

a b c d

Figure 1: Fits of (a) the Gamma distribution, (b) e^{a+bx}, (c) $e^{a+bx+cx^2}$, and (d) $e^{a+bx+cx^2+dx^3}$ to the log-linear distribution of 24-hour precipitation. The y-axis shows the log of the frequency and the x-axis the linear scale of precipitation amounts.

Both parameter estimates based on the moments (red) as well as the maximum likelihood (blue) estimators are shown in Figure 2. In general, the two types of estimators give similar features, however, the moments estimator tends to yield higher peak values for the scale parameter.

3.2.1 Geographical dependency of the scale parameter

Figure 3 shows how the scale parameter differ from location to location across Scandinavia (note that a threshold of 0.1mm was used here as opposed to 1mm in the other analyses). Panels a–d indicates an interesting a large-scale pattern with greater values in the southwest and lower values in the east for all seasons. There is no clear pattern in the shape parameter in Figure 4, and again, the results are similar for all the seasons. Figure 5 provides an illustration of how thew shape of the pdf depends on the scale and shape parameters. Dashed thin lines show the Gamma distributions for unrealistic hypothetical cases whereas thick curves are more representative for the actual rainfall amounts. Unrealistically large values for both scale and shape move the location of the distribution towards high values and lower the probability for drizzle.

Figure 6 shows the mean number of rainy days N for each season, and the general pattern is that N along the west coast of southern Norway is greater than in southeastern Norway. The number of rainy days in southern Sweden is also high and of the same magnitude as the Norwegian west coast.

3.2.2 Downscaling the Gamma parameters

The adjusted R^2 statistic for the downscaling of the shape and scale parameters (i) was 0.11 and 0 respectively (see Appendix B). The same statistic for their transform $\sqrt{\alpha}$ and $1/\beta$ (iii) was 0.14 and 0.04, hence slightly improved with respect to the straight-forward (traditional) downscaling. In comparison, the adjusted R^2 statistic for the (3-month) $\overline{x_R}$ and s (ii) was 0.16 and 0.09, suggesting that there was not much to be gained from downscaling $\overline{x_R}$ and s and subsequently calculate α and β. The low R^2-score for $\overline{x_R}$ contrast with the high values obtained when using more traditional seasonal means $\overline{x}$, suggesting that the number of rainy days n is more closely associated with the large-scale circulation than the amount that falls once it is raining. In summary, the downscaling analysis only indicated a weak relationship between the SLP and the shape parameters and no relationship with the scale parameter.

Systematic relationships can also be explored through spatial correlation analysis (Figure 7). The results from this kind of analysis shows that there is a strong connection between the number of rainy days (hence supporting the interpretation of the large-scale circulation influencing the number of rainy days rather than the actual amount) and the circulation pattern (here given as anomalies in the SLP, large-scale 2m temperatures or large-scale precipitation) and a weak association between the shape parameter and the circulation. The scale parameter, on the other hand, did not exhibit a correlation that was significant at the 5% level (no shading in Figure 7b).

Figures 8 and 9 show the correlation analysis with gridded temperature and precipitation. The correlation between temperature and the scale parameter suggests a region of association that is statistically significant at the 5% level south of Iceland, however, these may be due to chance according to the problem of multiplicity. It is expected that $\sim$5% of the area will show up as statistically significant at the 5% level. The effect of this type of field significance can also be seen in the correlation

analysis with the gridded precipitation in Figure 9 where small scattered regions spuriously show up as 'significant'.

The dependency of the Gamma parameters to local mean temperature and precipitation (here taken over the entire series) can be explored by a stepwise multiple regression analysis (Table 2 and 3) over the 49 locations shown in Figure 1. A regression analysis suggests that these parameters are indeed related to local mean temperature and precipitation as well as the number of rainy days (n). The ANOVA results of the step-wise regression analysis also indicates an association between the KS statistics (Kolmogorov-Smirnov) and both the shape parameter. The Kolmogorov-Smirnov (also known as the 'Lilliefors test') test statistic gives an indication of the similarity between the empirical and fitted distributions (worse fit gives higher shape values).

The scale parameter also exhibited associations with the altitude and distance from the coast (Table 3). The R^2 from the regression analysis was 0.89 for both the shape and scale parameter, suggesting a strong and systematic relationship between the Gamma parameters and the local climate type. These results suggest that deriving the Gamma parameters from the mean local temperature, precipitation as well as geographical information such as distance from the coast and altitude (vii) is a promising approach. However, it is interesting to note the fact that the quality of fit is one of the important parameters and that a worse fit (larger KS) gives lower estimates for shape but higher values for scale. The visual similarities between the various results in Figure 1 suggests that the for the Gamma distribution are comparable to those from the exponential law approach. We will therefore explore the exponential law approach more closely.

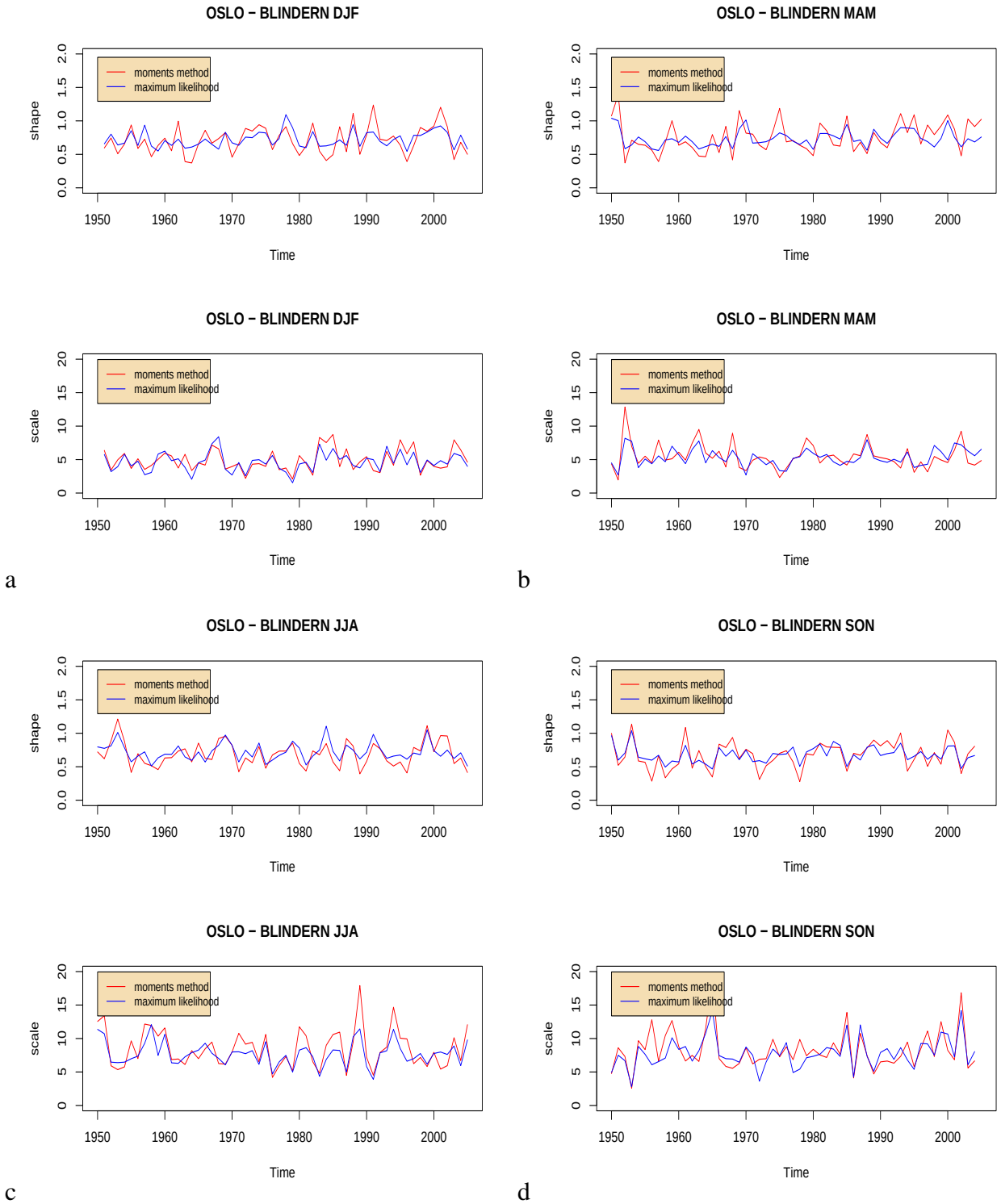

Figure 2: The temporal dependency of the shape and scale parameters in the best-fit Gamma distribution to 24-hour precipitation in Oslo for different seasons. Red curve represents the moments estimators and blue the maximum likelihood estimations.

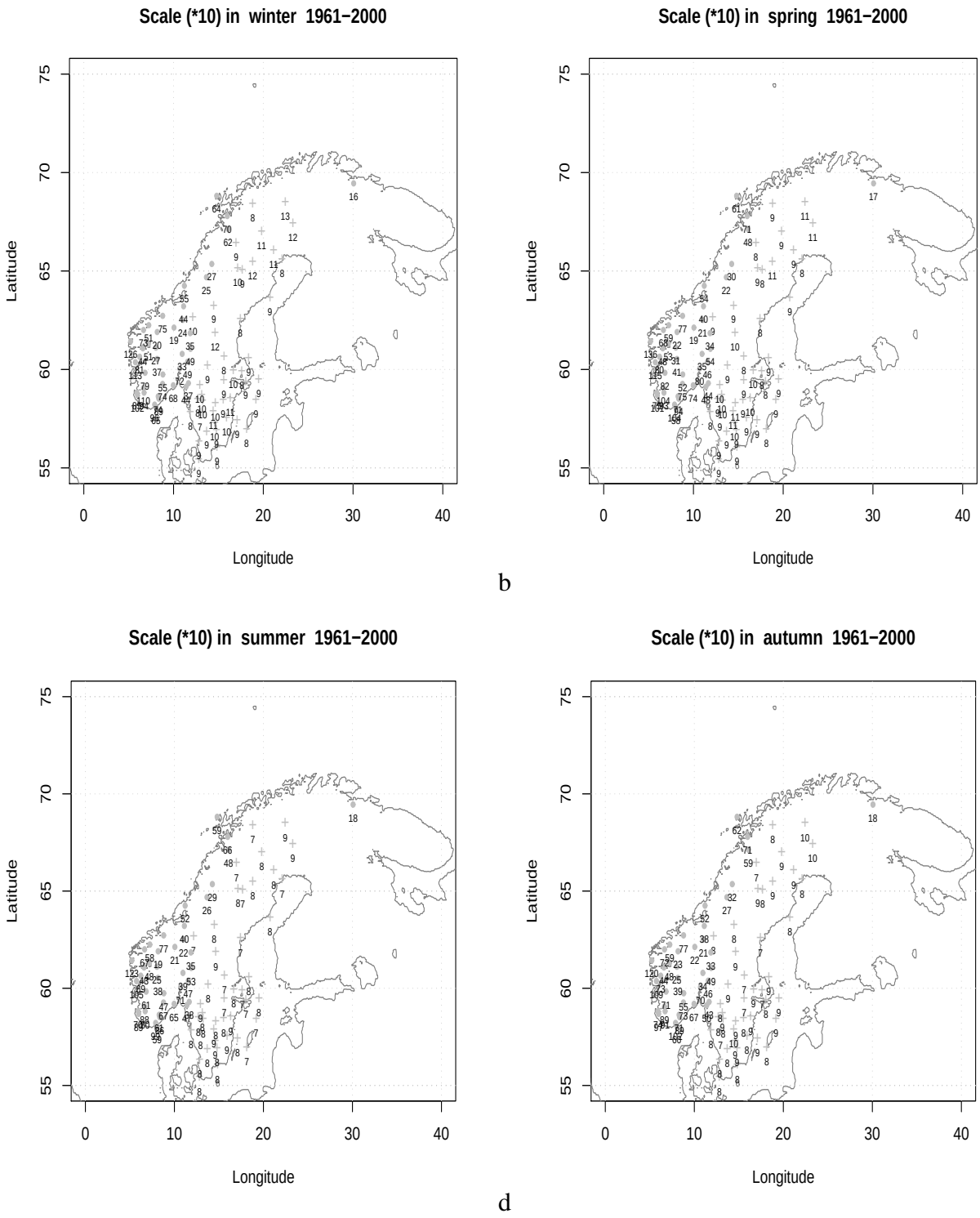

Figure 3: Estimates of how the maximum likelihood estimates for scale parameter varies with location. The four panels show the results for December–February (a), March–May (b), June–August (c) and September–November (d). The Gamma distribution was fitted precipitation amounts for days exceeding 0.1mm.

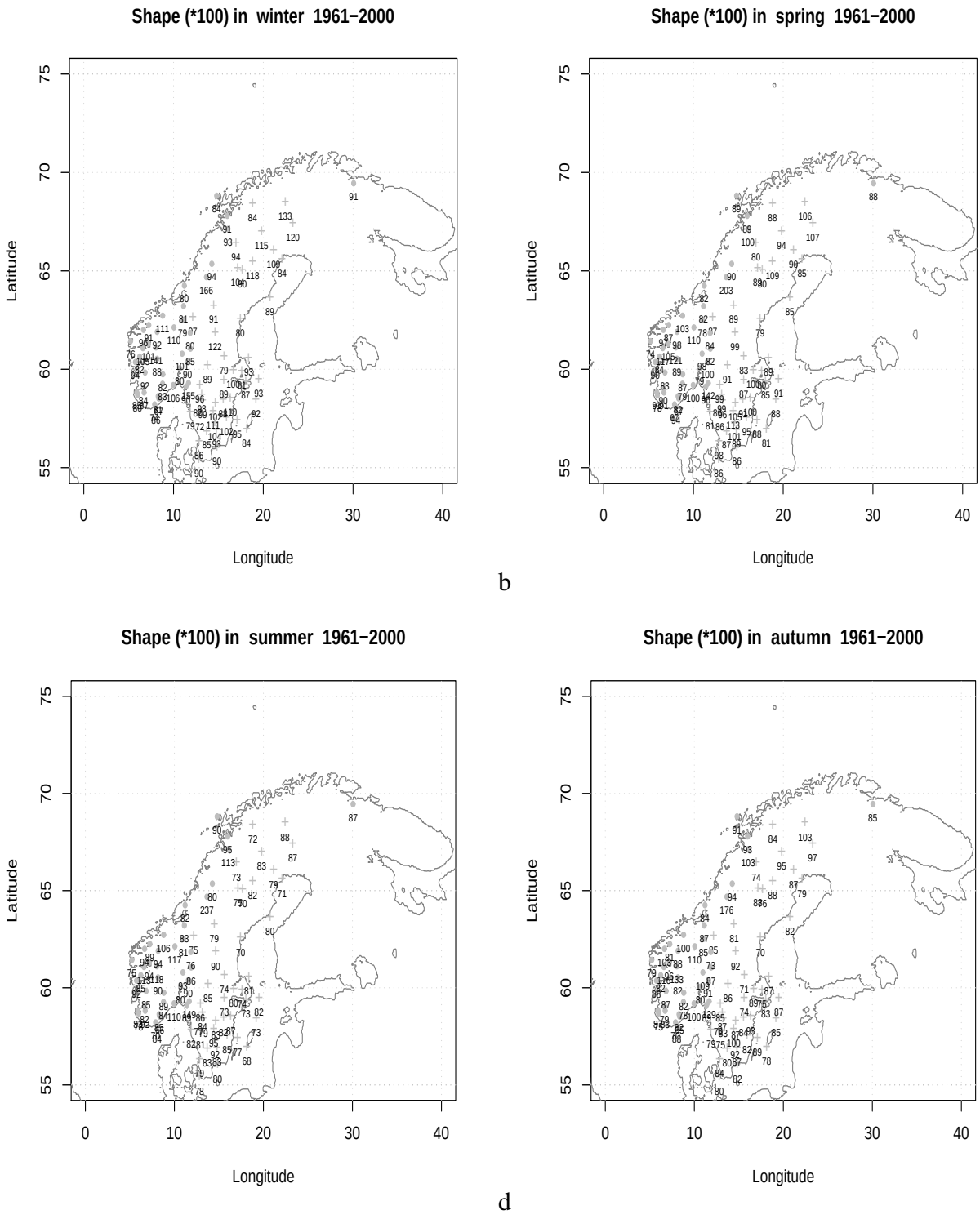

Figure 4: Estimates of how the maximum likelihood estimates for shape parameter varies with location. The four panels show the results for December–February (a), March–May (b), June–August (c) and September–November (d). The Gamma distribution was fitted precipitation amounts for days exceeding 0.1mm.

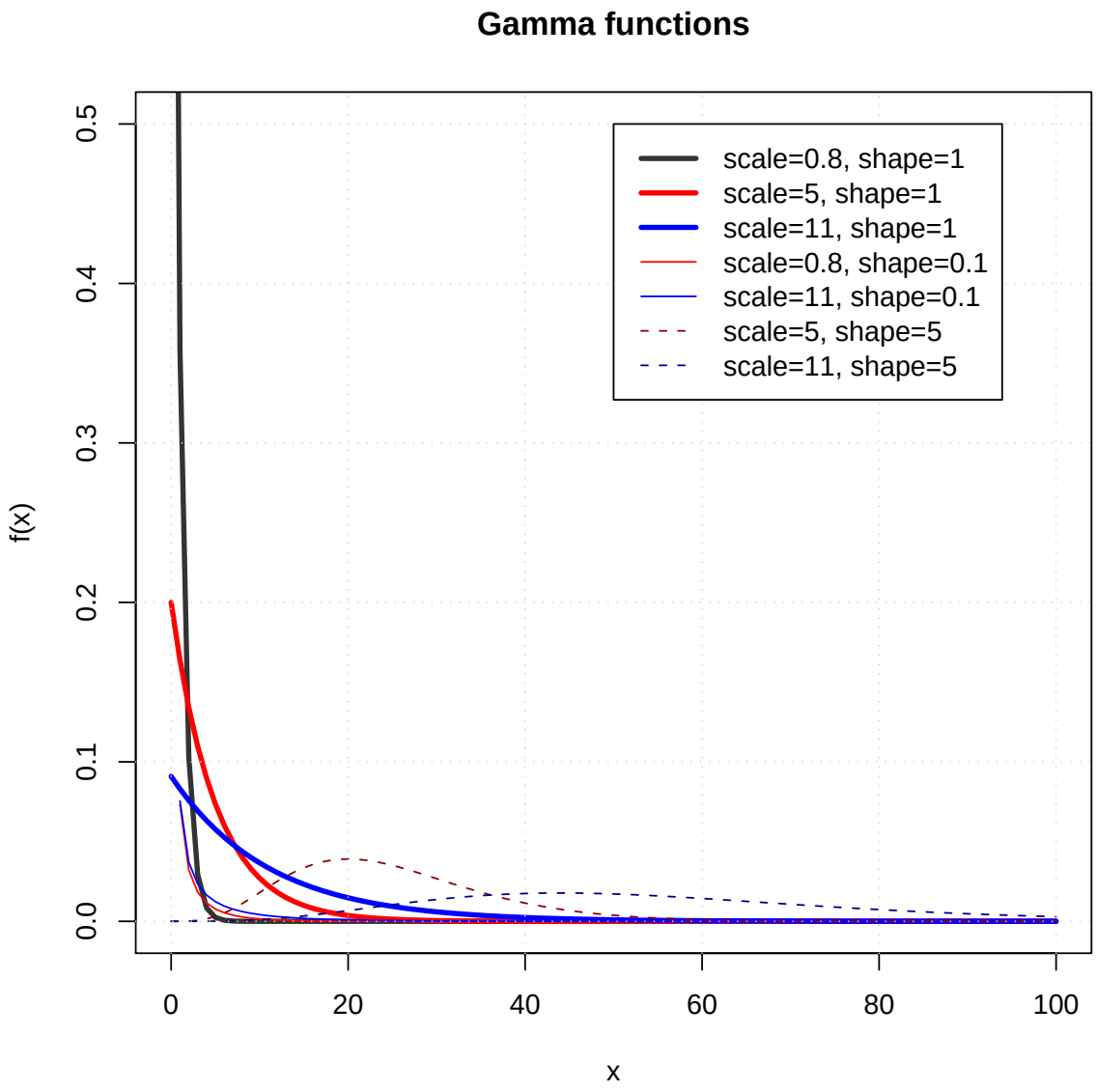

Figure 5: Illustration of how the shape of the Gamma function varies with values for shape and scale.

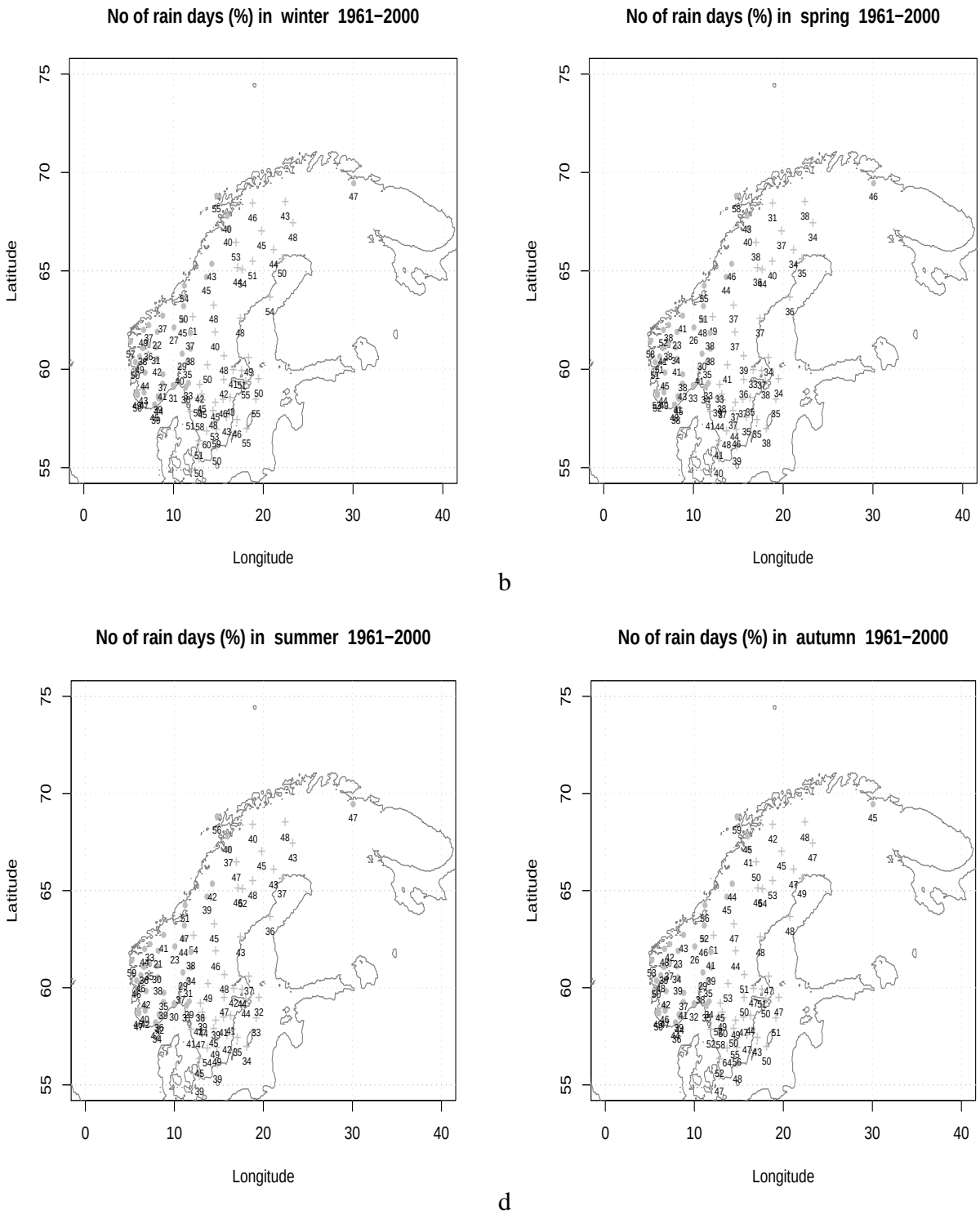

Figure 6: Estimates of how the number of rainy days varies with location. The four panels show the results for December–February (a), March–May (b), June–August (c) and September–November (d). The threshold for a rainy day was rainfall greater than 0.1mm.

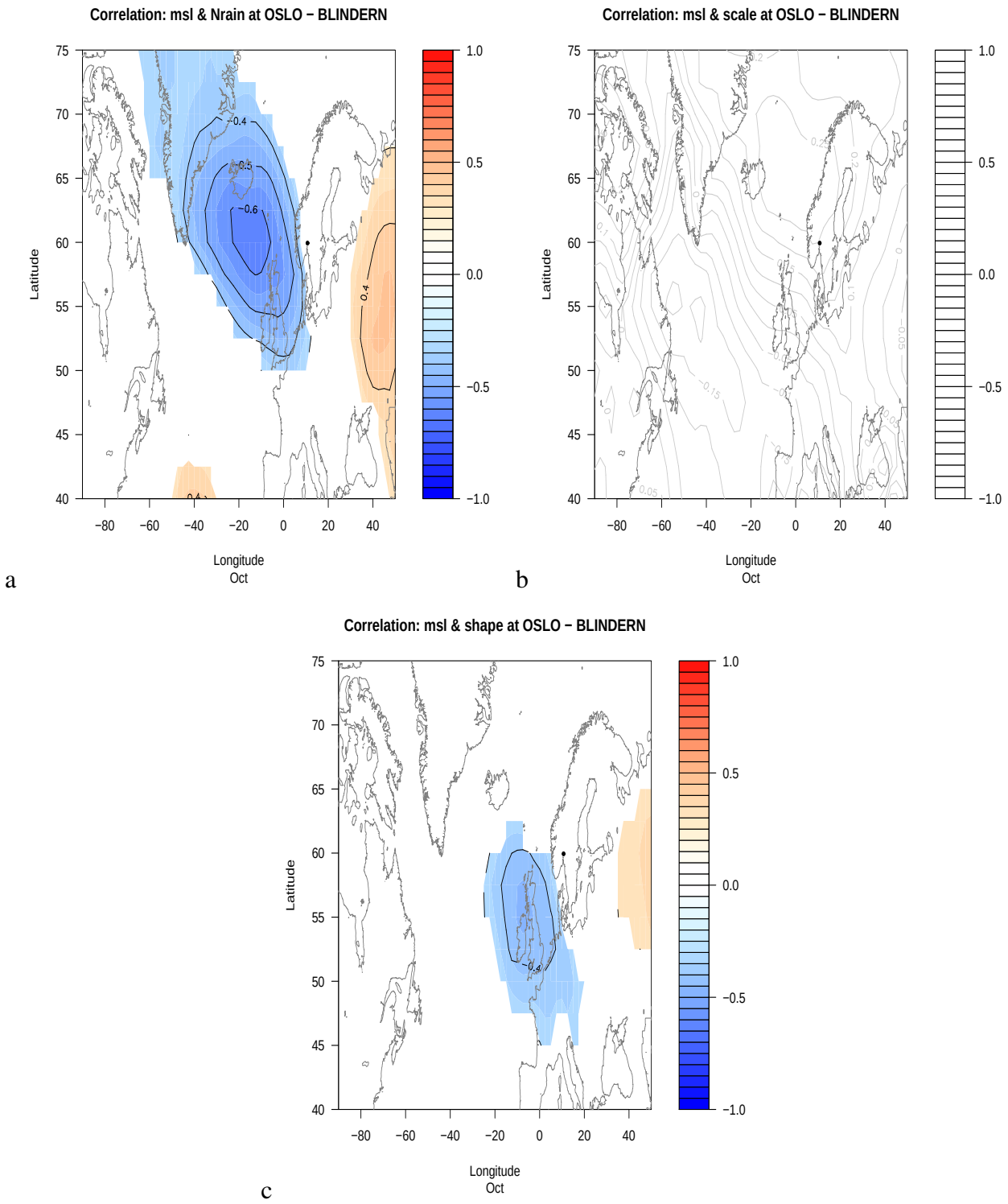

Figure 7: Correlation maps showing the correlation between SLP and (a) number of rainy days in Oslo, the scale (b) and the shape (c) parameters for the Oslo precipitation distribution. Only the shaded areas show correlation values that are statistically significant at the 5% level.

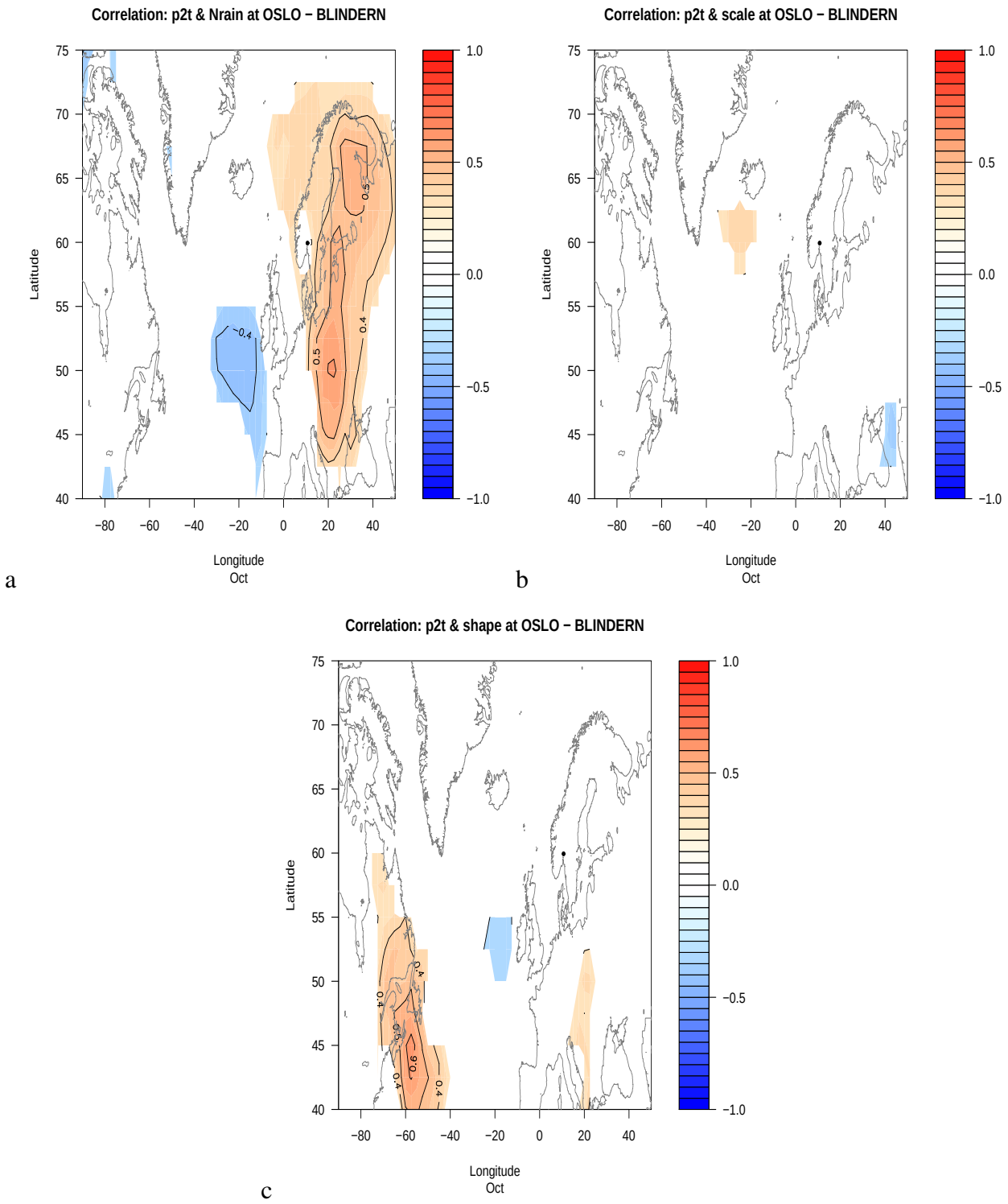

Figure 8: Correlation maps showing the correlation between large-scale T(2m) and (a) number of rainy days in Oslo, the scale (b) and the shape (c) parameters for the Oslo precipitation distribution. Only the shaded areas show correlation values that are statistically significant at the 5% level.

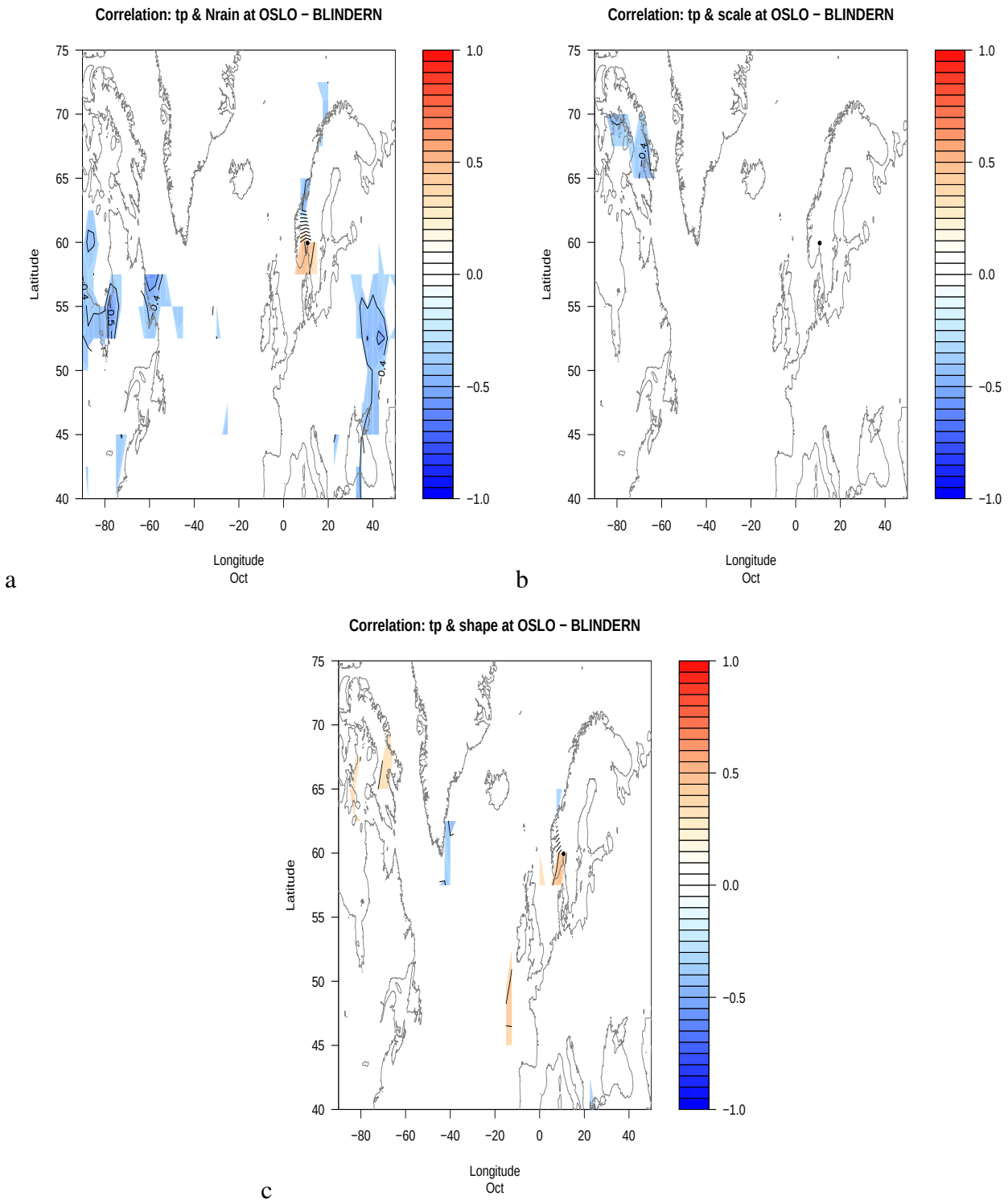

Figure 9: Correlation maps showing the correlation between large-scale precipitation and (a) number of rainy days in Oslo, the scale (b) and the shape (c) parameters for the Oslo precipitation distribution. Only the shaded areas show correlation values that are statistically significant at the 5% level.

shape

	Estimate	Std. Error	t value	Pr($>\|t\|$)
(Intercept)	1.481e+00	5.530e-02	26.787	$<$ 2e-16 ***
temp	-1.641e-02	2.419e-03	-6.785	2.36e-08 ***
precip	-4.984e-02	1.975e-02	-2.523	0.0153 *
n	1.089e-05	6.183e-06	1.762	0.0850 .
KS	-2.146e+00	1.556e-01	-13.789	$<$ 2e-16 ***

Signif. codes: 0 '***' 0.001 '**' 0.01 '*' 0.05 '.' 0.1 ' ' 1

Table 2: Residual standard error: 0.1122 on 44 degrees of freedom, Multiple R-Squared: 0.8854, Adjusted R-squared: 0.875, F-statistic: 85.01 on 4 and 44 DF, p-value: $<$ 2.2e-16.

scale

	Estimate	Std. Error	t value	Pr($>\|t\|$)
(Intercept)	-1.209e+01	2.010e+00	-6.016	3.77e-07 ***
temp	5.952e-01	9.417e-02	6.321	1.37e-07 ***
precip	3.390e+00	7.205e-01	4.704	2.76e-05 ***
alt	4.037e-03	1.481e-03	2.725	0.00933 **
dist	-1.791e-02	7.995e-03	-2.240	0.03042 *
n	-5.716e-04	2.327e-04	-2.456	0.01827 *
KS	8.276e+01	5.749e+00	14.395	$<$ 2e-16 ***

Signif. codes: 0 '***' 0.001 '**' 0.01 '*' 0.05 '.' 0.1 ' ' 1

Table 3: Residual standard error: 4.039 on 42 degrees of freedom, Multiple R-Squared: 0.8897, Adjusted R-squared: 0.8739, F-statistic: 56.45 on 6 and 42 DF, p-value: $<$ 2.2e-16.

In summary, the scale parameter exhibited a geographical dependency with greater values along the coast of southwestern Norway, but showed little association with the type of large-scale circulation (Oslo only). The shape parameter, on the other hand, revealed no systematic dependency to the geography but estimate for Oslo indicated a relationship with low pressure over the British Isles.

3.3 Exponential distribution

One advantage with a simple exponential distribution $f(x) \propto e^{mx}$, where $m < 0$, is that any percentile q_p can easily be derived analytically given the slope m:

$$q^*_{0.95} = \log(1-p)/m \tag{8}$$

(see the appendix A). The pdf can be written as $f(x) = me^{-mx}$ because

$$F(x) = \int_{x=0}^{\infty} f(x)dx = \int_{x=0}^{\infty} -me^{mx}dx = 1. \tag{9}$$

Here, we use $f(x)$ to describe rainy days only and dry days have been removed prior to the analysis. It can also be shown that

$$\overline{x_R} = \int_{x=0}^{\infty} mxe^{-mx}dx = -\frac{1}{m}, \tag{10}$$

where $m < 0$. This expression is convenient because it allows an estimation of the higher percentiles based on the mean value and the number of rainy days since $\hat{m} = \frac{1}{\overline{x_R}} - 1$. It is possible to take this further and use this expression together with equation 8 to express the 95% percentile in terms of $\overline{x_R}$:

$$q^*_{0.95} = \frac{\log(1-p)}{\frac{1}{\overline{x_R}} - 1} \tag{11}$$

Here, the following convention will used: q_p represente the true theoretical value, whereas $q^*_{0.95}$ represents the solution to the analytical expression given in equation 8, and $\hat{q}_{0.95}$ the empirical estimated percentile. Likewise, $\hat{m}$ denotes a estimated value and m is a theoretically true value. Figure 10 shows a comparison between values given by the analytical expression 8 and the empirical values (filled circles).

Figure 10 suggests that the simple exponential model generally gives a reasonable good representation of the upper tail of the distribution and that $f(x) = -me^{\hat{m}x}$ provides an approximate description of the rainfall amount distribution for the rainy days. Whereas the data from the Norwegian stations (black) indicate a good agreement between analytical and empirical results (points scattered along a linear line parallel to the diagonal), the ECSN data (grey points) exhibit a somewhat greater scatter between $q^*_{0.95}$ and $\hat{q}_{0.95}$. The use of third-order polynomial model for the log-linear slope (open circles) did not produce a better correspondence than the simpler $f(x) = -me^{\hat{m}x}$.

Tables 4 and 5 list the statistics for the skill of predicting the slope m and constant c in $f(x) = e^{c+\hat{m}x}$ from the local mean temperature, precipitation, altitude, distance from the coast (in km), the number of rainy days (n) and the goodness of fit of the local distribution model to the empirical data r^2 (this is the same kind of R^2-statistic as presented in this multiple regression analysis, but is for

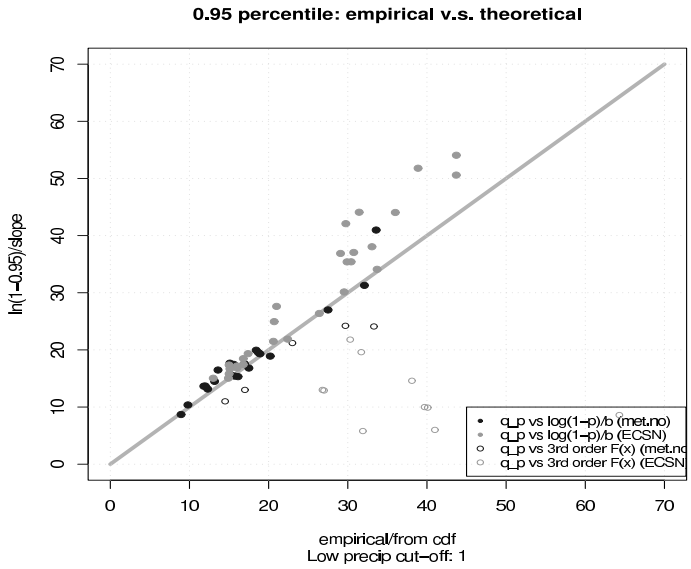

Figure 10: Comparison between modelled and empirical values for the 95% percentiles (for rainy days only). The filled circles show how well the empirical estimates of $q_{0.95}$ correlate with $q^*_{0.95}$ for the station data from the Norwegian Meteorological Institute (black) and ESCN (grey) respectively. The open circles are shown below the axis (mirrored) and represent percentile derived using the exponential expression $f(x) = e^{c+\hat{m}_1 x+\hat{m}_2 x^2}$.

the linear regression analysis used to estimate the slope $\hat{m}$). The high R^2 statistics (0.86 and 0.90 respectively) are in line with previous results derived for the Gamma model and indicate a strong dependency between these parameters and the local climate type. The dependency of the slope and constant parameters to the quality of linear fit is also similar to the results for the Gamma distribution, here represented by the r^2 rather than the KS-statistics. A worse fit tends to give lower values for the slope but higher values for the constant. However, when working with pdfs, it is the slope that matters as the curves are scaled so that the area under the curve is one: $f(x) = -me^{mx}$ ($m < 0$).

Figure 11 shows predicted distribution functions for four locations *not included in the regression analysis* - thus representing independent realisations. These results suggest that it is possible to get an approximate representation of the daily precipitation distribution for an independent location, given the local mean temperature, precipitation, number of rainy days and altitude (r^2 was excluded from the prediction model, since we do not know in advance how well the fit would be if we didn't have the data). The second order exponential expression $f(x) = e^{c+m_1 x+m_2 x^2}$ was used for 3 of the four locations, but a second-order fit would yield a poor representation for Teigahorn (here represented by $f(x) = -\hat{m}e^{\hat{m}x}$ where $\hat{m} < 0$). Furthermore, the comparison between $f(x)$ (black dash/solid lines) and the histograms (grey symbols) indicate a failure to account for the fat tail in some accounts (Teigahorn and Tortosa).

It is also possible to apply the regression results to prediction of temporal changes. Figure 12

slope

	Estimate	Std. Error	t value	Pr($>\|t\|$)
(Intercept)	2.101e-01	9.013e-02	2.332	0.02436 *
temp	5.529e-03	6.005e-04	9.207	8.02e-12 ***
precip	2.560e-02	3.247e-03	7.886	5.89e-10 ***
alt	2.264e-05	7.916e-06	2.860	0.00645 **
r^2	-4.860e-01	9.674e-02	-5.024	8.91e-06 ***

Signif. codes: 0 '***' 0.001 '**' 0.01 '*' 0.05 '.' 0.1 ' ' 1

Table 4: Residual standard error: 0.02446 on 44 degrees of freedom, Multiple R-Squared: 0.8566, Adjusted R-squared: 0.8436, F-statistic: 65.73 on 4 and 44 DF, p-value: $<$ 2.2e-16.

const

	Estimate	Std. Error	t value	Pr($>\|t\|$)
(Intercept)	2.854e+00	6.683e-01	4.271	0.000105 ***
temp	-4.135e-02	4.312e-03	-9.588	3.05e-12 ***
precip	-2.234e-01	2.525e-02	-8.849	3.08e-11 ***
alt	-1.593e-04	5.959e-05	-2.673	0.010580 *
n	1.342e-05	9.873e-06	1.359	0.181308
r^2	5.474e+00	7.257e-01	7.542	2.13e-09 ***

Signif. codes: 0 '***' 0.001 '**' 0.01 '*' 0.05 '.' 0.1 ' ' 1

Table 5: Residual standard error: 0.1756 on 43 degrees of freedom, Multiple R-Squared: 0.8961, Adjusted R-squared: 0.884, F-statistic: 74.19 on 5 and 43 DF, p-value: $<$ 2.2e-16.

shows the prediction (extrapolation) of variation of the seasonal 24-hour precipitation distribution in Oslo and Bergen with a 2nd order polynomial and linear exponential models respectively. The model underestimates the frequency of days with low precipitation in Bergen during winter and autumn, but yields an approximate representation of the distribution functions for Oslo. Part of the discrepancy between empirical and extrapolated representation is associated with the constant value not used in the estimation of the pdf. Here, the probability densities are used along the y-axis, and since these are significantly less than 1 small errors tend to appear more serious than a linear plot would indicate. The extrapolated pdfs in the main frame show a better correspondence with the empirical data. Especially the curve for the autumn in Bergen (grey) indicates too low occurrence of drizzle and too many cases with heavy precipitation. Bergen has a climate type that is very distinct to that of most other stations used in this study to train the statistical models presented in Tables 4 & 5. Different mechanisms, such as predominant orographically forced rainfall in Bergen but absent in other locations, may render the extrapolations invalid for special places like Bergen.

In summary, extrapolations based on the regression analysis and predictions using the mean temperature and precipitation suggest that there is some merit in exponential law approach, although there are some cases which are not well-represented by this method. Some possible explanations for the failure of the models may be that important information may be missing in the predictions or that the statistical relationship is non-stationary with respect to magnitude, location or time. Furthermore, there is no guarantee that the statistical models are representative for all locations, and care must be taken when selecting locations for model calibrations. In the next section the Gamma and exponential law approaches are compared with more traditional ways of downscaling precipitation for some extreme historical cases.

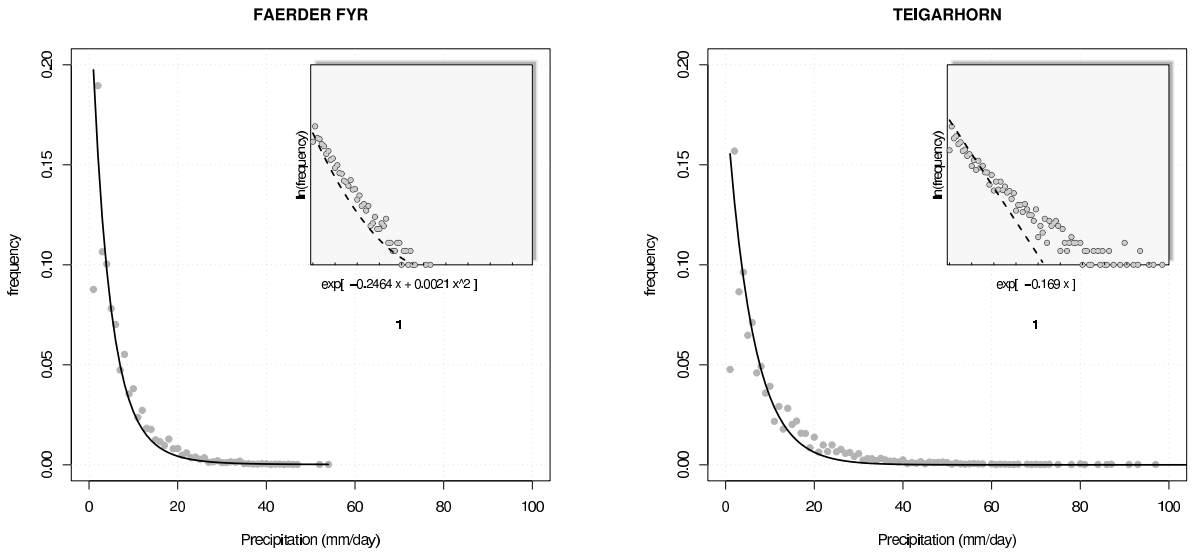

a

b

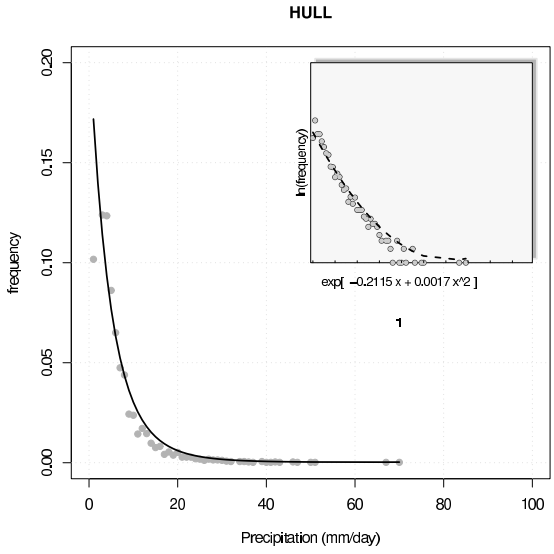

c

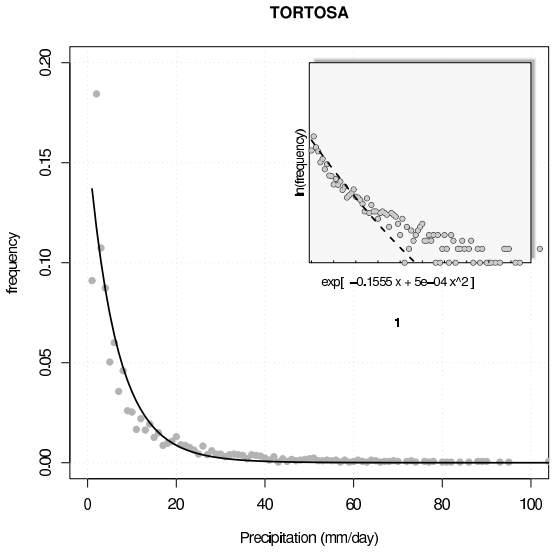

d

Figure 11: Predicted distribution functions for 4 locations not used in the calibration. The inserts show the semi-log plots with grey sympols representing the empirical values (histograms) and dashed black lines the best-fit $f(x)$. Main figures show curves corresponding to the pdf (black curve) and histograms (grey symbols).

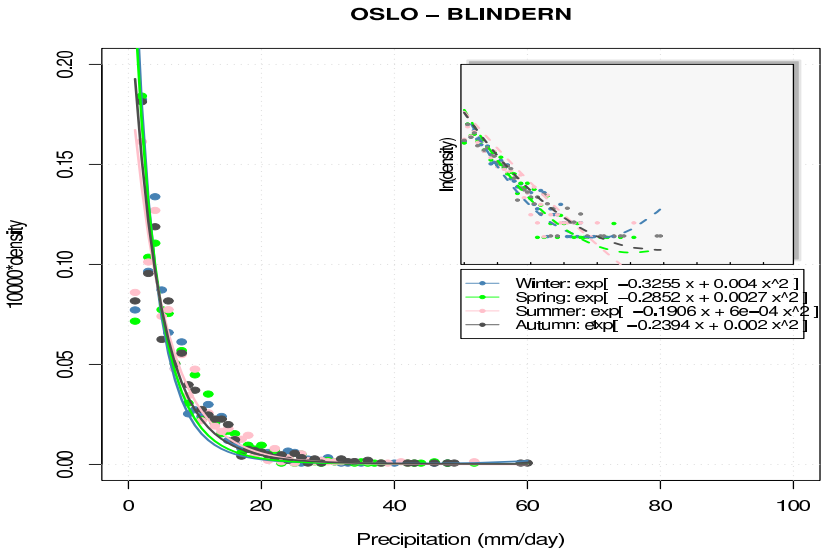

a

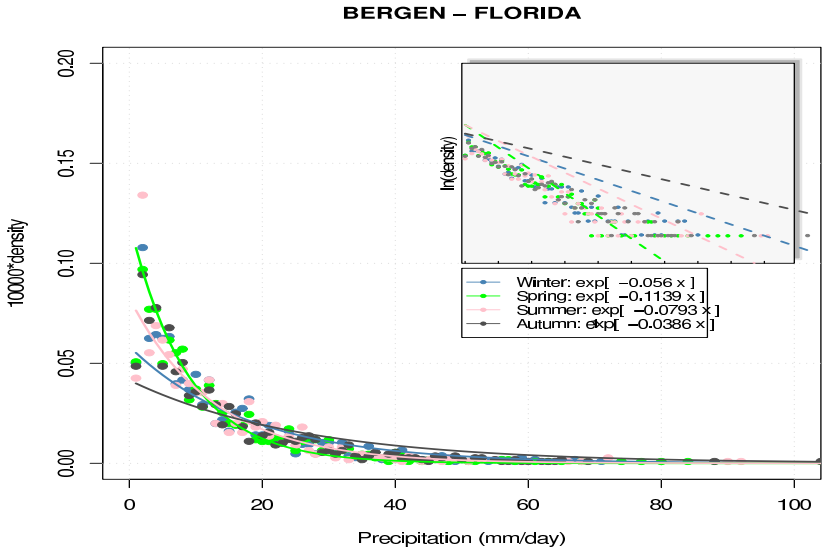

b

Figure 12: Seasonal dependency: lines represent estimates for $f(x)$ and symbols represent the empirical values. The different seasons are shown in different colours.

3.4 Case study: autumn 2000

Autumn 2000 was extreme in terms of precipitation, with unprecedented amounts of rainfall over southeastern Norway in November and an autumn season with unusually many rainy days (*Benestad & Melsom*, 2002). It is often such extreme events that are most interesting in terms of future climate scenarios, and therefore we will use September–November as a case study here for testing the downscaling of Gamma parameters.

Figure 13 shows the empirical distributions and Gamma fits for the autumn 2000 24-hour precipitation for (a) Bjørnholt near Oslo, (b) Oslo-Blindern, (c) Bergen-Florida, and (d) Tromsø. Both the moments (red) and maximum likelihood (blue) estimators were used for fitting the pdf, however, the difference between these were marginal. It is evident that the Gamma distribution does not capture the large number of heavy precipitation.

Figure 14 shows a comparison between various downscaling efforts for predicting the local distribution function for 24-hour precipitation in Oslo, based on SLP (a), T(2m) (b) and large-scale precipitation. Also shown are distribution functions based on the exponential law and the regression analysis above and from analog and linear downscaling of daily values. The histogram for the 24hr precipitation during autumn 2000 has an irregular shape, which cannot be reproduce by the Gamma or exponential law distributions. Although the analog model in theory doesn't have a constraint in terms of the shape of the distribution, it did fail to capture the upper tail of the histogram. According to Figure 13, the exponential law distributions gave the closest description of the rainfall distribution for autumn 2000 despite the constraints regarding shape.

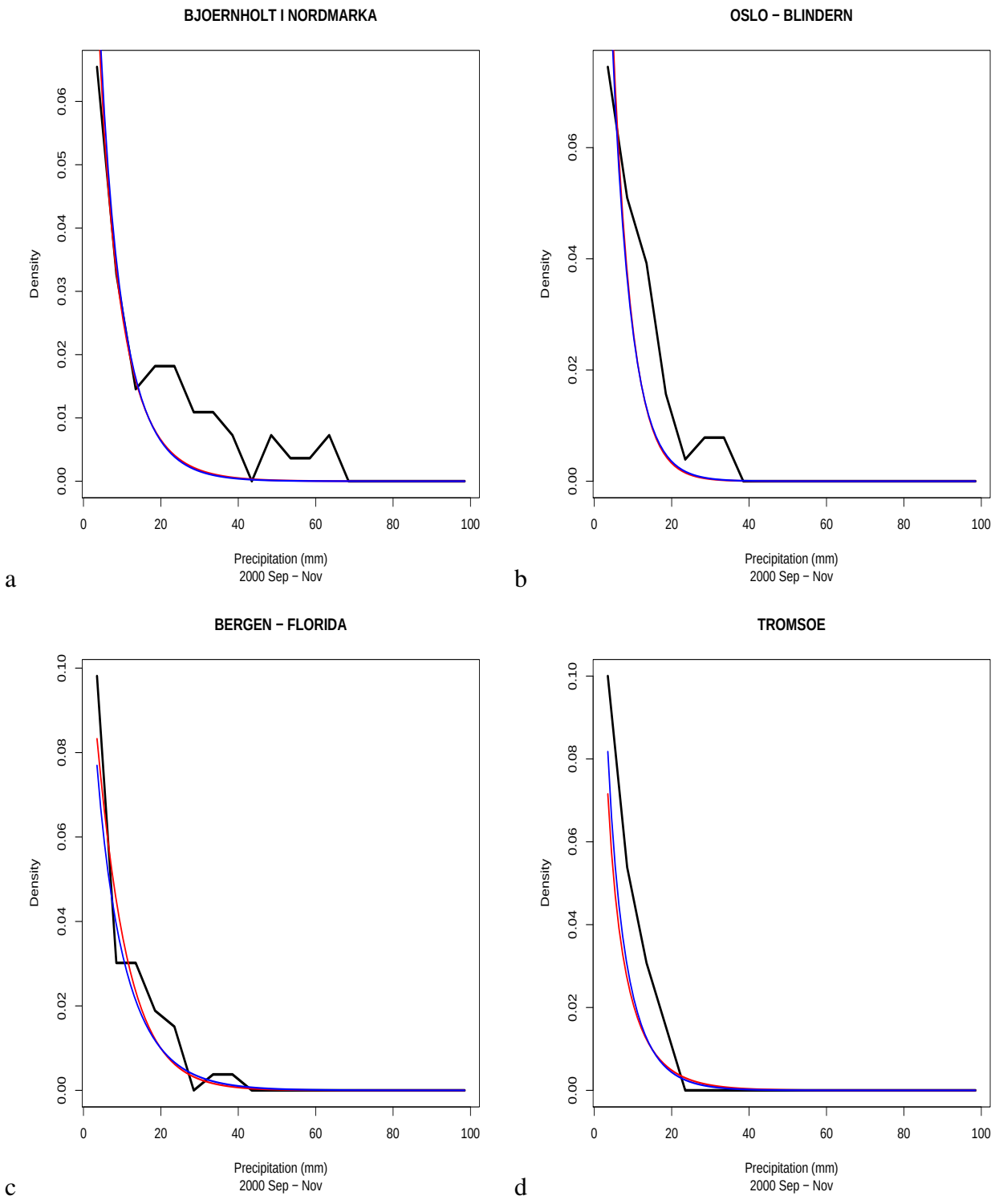

Figure 13: Frequency distribution of 24-hour rainfall for September–November 2000. Black lines represent the observed histograms and red and blue curves show the best-fit Gamma distributions (red= moments estimators, blue=maximum likelihood estimators).

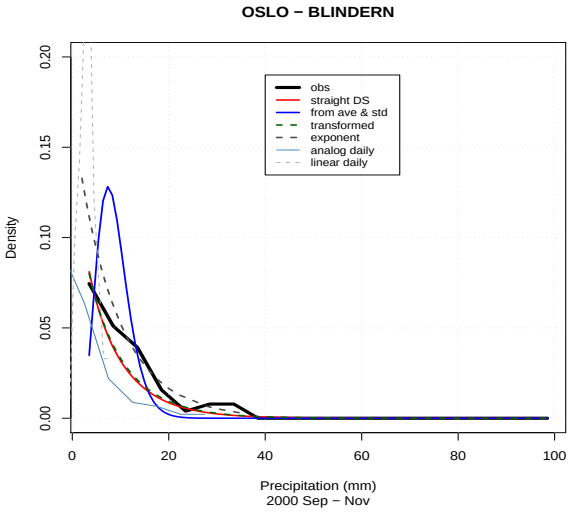

a

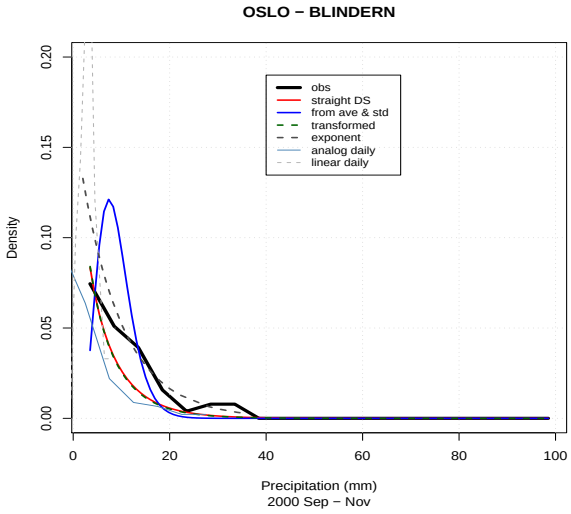

b

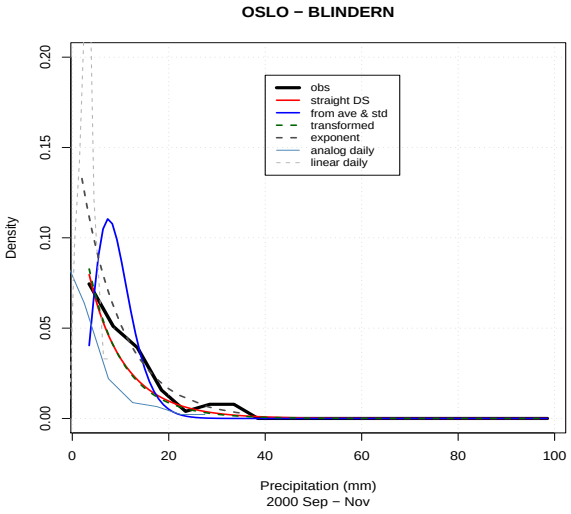

c

Figure 14: Inter-comparison of results derived for Oslo through various strategies for September–November 2000. Panels a–c show downscaled Gamma parameters based on SLP, temperature and precipitation respectively.

4 Record-statistics

A test was applied to an arbitrary selection of data series to examine whether the 24hr precipitation series were consistent with the data being independent and identically distributed (iid) and weather the use of standard GEV and analog models, which assume a stationary pdf or a fixed range of values, are appropriate. The iid-test is discussed in *Benestad* (2004b, 2003). The computer code for performing this test is now available as an `R`-package (iid.test) on CRAN, and the results of the analysis are presented in Figure 15.

The signature of a non-iid process is when the empirical (counted) number of record-events ($\hat{\mathcal{E}}(n)$ represented as symbols) falls outside the confidence region (grey shaded region). The theoretical expected number of records $\mathcal{E}(n) = \sum_{i=1}^{n} 1/i$ is represented by the diagonal solid line in the figure (shown with an exponential scaling of the ordinate). The iid-test can be applied to a series in the chronological order or the reversed chronological order, and for iid data the results are expected to be similar either way. If the 'forward' and 'backward' analyses diverge and fall on either side of the confidence region, then this is a sign of the data being non-iid. Missing data will result in a low bias for both 'forward' and 'backward' analyses. The same is true for series of daily rainfall amounts with a number of dry days. Nevertheless, the biases of missing values or dry days can only lead to under-count and a false rejection of the alternative hypothesis, thus being conservative in terms of rejecting the null-hypothesis. The iid-test indicates a low number of record-events for some locations both for 'forward' and 'backward' order (Perginan, Tortosa). The locations with low counts are associated with climates where the number of rainy days is low and with a high portion of dry days. In fact, series with a small fraction of rainy days are likely to give an under-count of record-events according to this iid-test where all the days count, also the dry ones. It is conceivable that there is an ongoing trend in a location where it rains 1 out of hundred days, and each time it rains, it breaks an old record. In this situation, the iid-test would fail to capture the signal at the early stage, but given a sufficiently long interval, the 'forward' counts would eventually catch up and surpass the theoretical estimate.

The results shown in Figure 15 do not indicate strong divergence between the 'forward' and 'backward' analyses, and the values for $\hat{\mathcal{E}}(n)$ tend to lie within the 95% confidence interval (grey shaded region). There are some exceptions to this rule such as Perginan and Tortosa, where both 'forward' and 'backward' analyses indicate values below the confidence region. These results are therefore biased by a large number of dry days. In some cases, one of the analyses stops after a short time due to missing values (cumulative sums of missing values gives a 'not-a-number' flag). These results do therefore not provide evidence of non-iid processes, and hence provide some justification to using analog models. There are no indications of anomalously high occurrence of record-breaking 24hr precipitation amounts or the distribution of these being stretched.

5 Future projections

An extrapolation of the exponential law was used to make projections for the future. The linear rate of change (°C per decade and mm/month per decade) in the local mean temperature and precipitation was taken from the downscaling analysis of *Benestad* (2005). These rates were multiplied by 6.5

in order to provide an estimate for the ΔT and Δprecipitation for year $\sim$2070. The scenarios are presented in Figure 12.

In some locations such as Oslo (Norway), Tromsø (Norway), De Bilt (The Netherlands), the results indicate little changes, whereas in places like Tranebjerg (Denmark) and Karlstad (Sweden), the extrapolation indicates a moderate increase the frequency of heavy 24hr-precipitation. There are also some cases, where the analysis point to substantial increase in extreme precipitation, including Helsinki (Finland), Bergen (Norway) and Glomfjord (Norway). However, it is important to keep in mind the facts that these results may be subject to biases and that the validations using independent data suggest that these extrapolations are not always accurate for all locations. The projections for Bergen and Glomfjord with a decrease in the days with drizzle and more dry days are considered not reliable since the physical situation for Bergen and Glomfjord with a dominance of orographically forced rainfall differs much from most other places, and hence an extrapolation based on other types of conditions (with a warmer climate but where the orographic effect on rainfall is absent) can produce misleading results. This interpretations is supported by failure of predicting the seasonal distributions for Bergen (Figure 12b). These results may nevertheless give an indication of changes that can be expected in the distribution functions for a number of locations for which the local orography does not play a special role. These results suggest that a future warming and a trend towards a wetter climate can also lead to more heavy precipitation events.

6 Discussion & Conclusions

The Gamma approach suggested that the scale parameter was not sensitive to the large-scale circulation, but both the number of rainy days and the shape parameter exhibit a relationship with the circulation pattern. The scale parameter exhibited a systematic dependency to geographical parameters. This information is useful for making future projections about changes in the pdfs for the 24-hr precipitation. The Gamma approach is suitable for downscaling the shape parameter directly for a given time interval (eg a season), and the downscaled parameters can be used in a weather generator for further studies. It is also possible to use multiple regression analysis against local climate characteristics such as local mean temperature and precipitation to make future projections for the pdfs. The downscaling of pdf parameters provide an indication of the shape of the distributions, but does not give information about the number of rainy days and hence the monthly means ($\overline{x}$). Additional downscaling of the number of rainy days (N) is required in order to get a complete picture of the rain characteristics for a given location.

The exponential-law approach points to highly statistical significant relationships between the slope parameter and the local mean temperature and precipitation that can be utilised in local climate change studies. The slope of the log-linear relationship between frequency (density) and amount can be utilised for simple estimates of quantiles. This approach is also suitable for providing inputs to weather generators.

There are some caveats associated with the downscaling of the distribution functions. Not all locations have rainfall characteristics that can be inferred from other locations and dependencies with local mean temperature and mean rainfall.

An extrapolation for the future based on a downscaling analysis of a multi-model climate model ensemble points to increased frequencies of days with moderate-to-heavy precipitation. The present statistical models are too inaccurate for representing the extreme values. A set of iid-test for the past rainfall records did not reveal evidence for changes in the upper range of the precipitation amount. However, one shortcoming of this analysis was that sunny days (no rain) tend to cause an under-count bias, and subsequent analysis with these considerations taken into account is required to resolve the question of past trends.

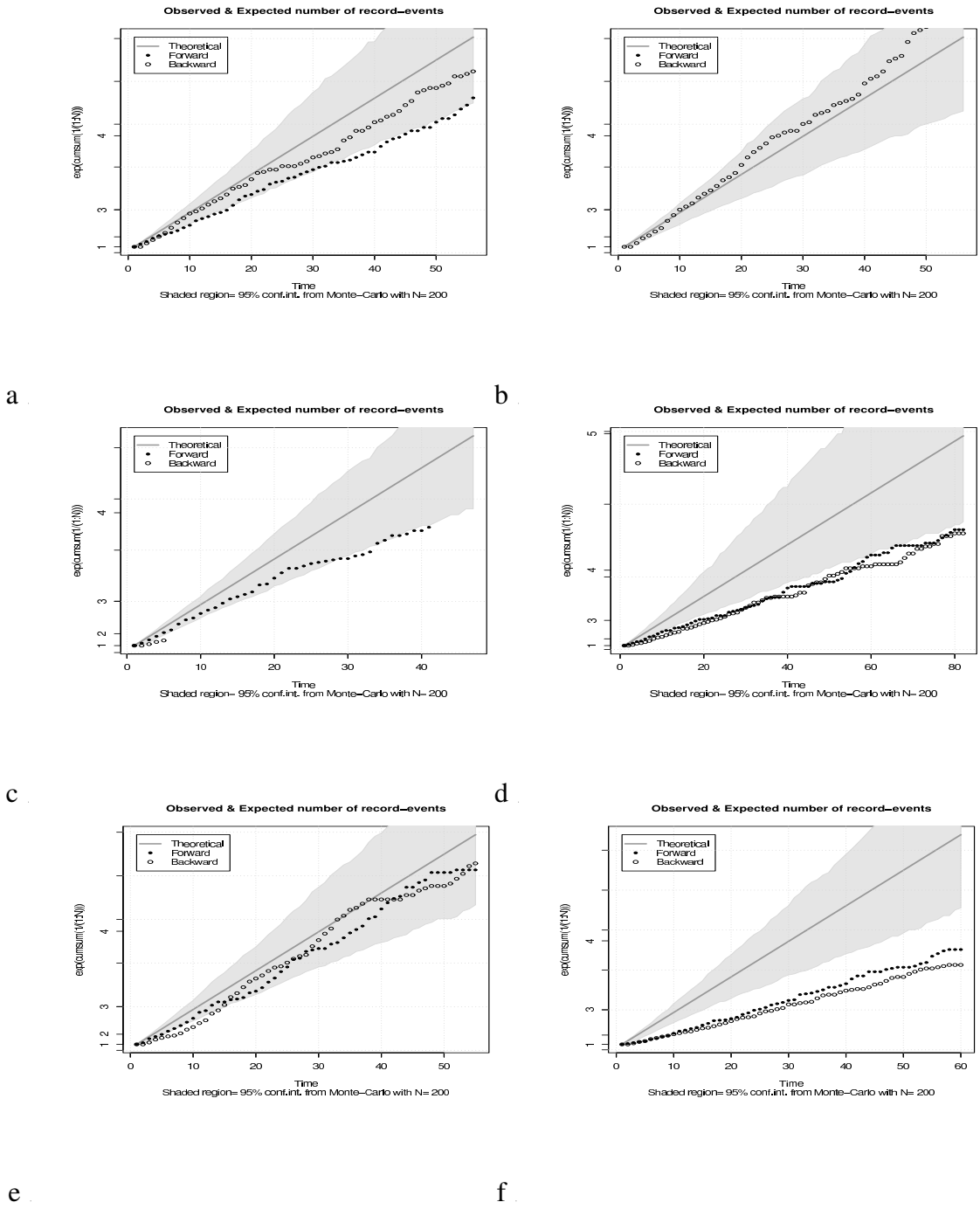

Figure 15: An results from an iid-test applied on 24hr precipitation from (a) Bjørnholt, (b) Ferder, (c) Hull, (d) Perginan, (e) Teigahorn and (f) Tortosa. The daily series have been sub-sampled every 5 day in order to reduce temporal correlation (dependencies).

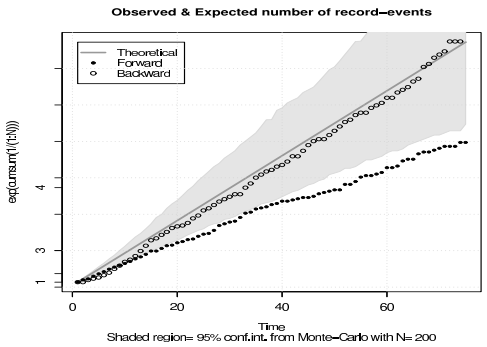

g

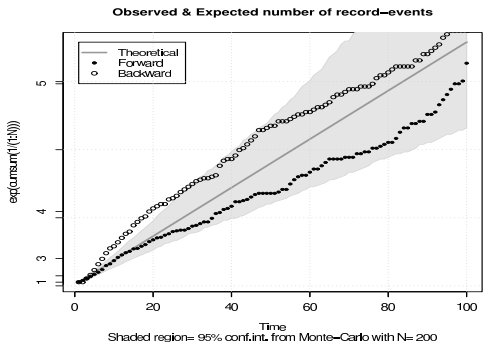

h

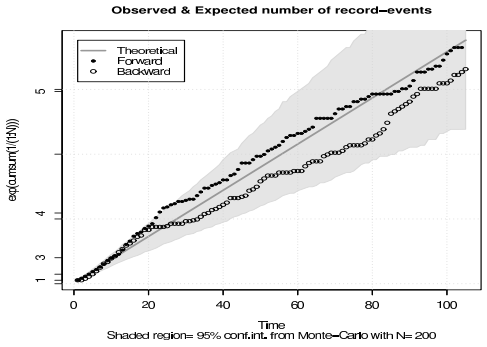

i

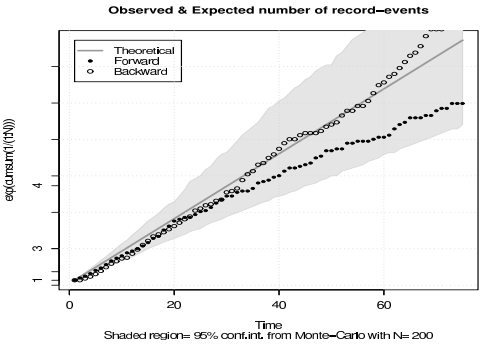

j

Figure 11: Figure 15 continued for (g) Armagh, (h) De Bilt, (i) Saentis, and (j) Oxford.

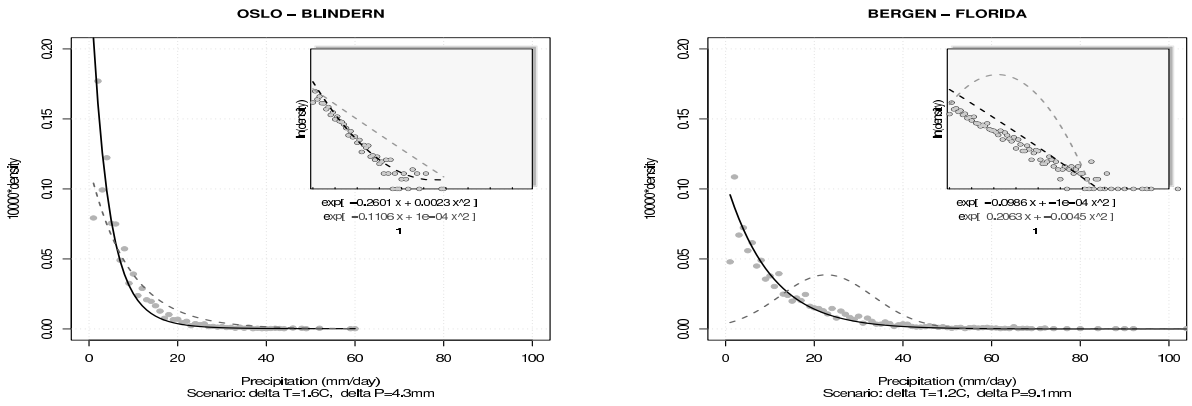

a b

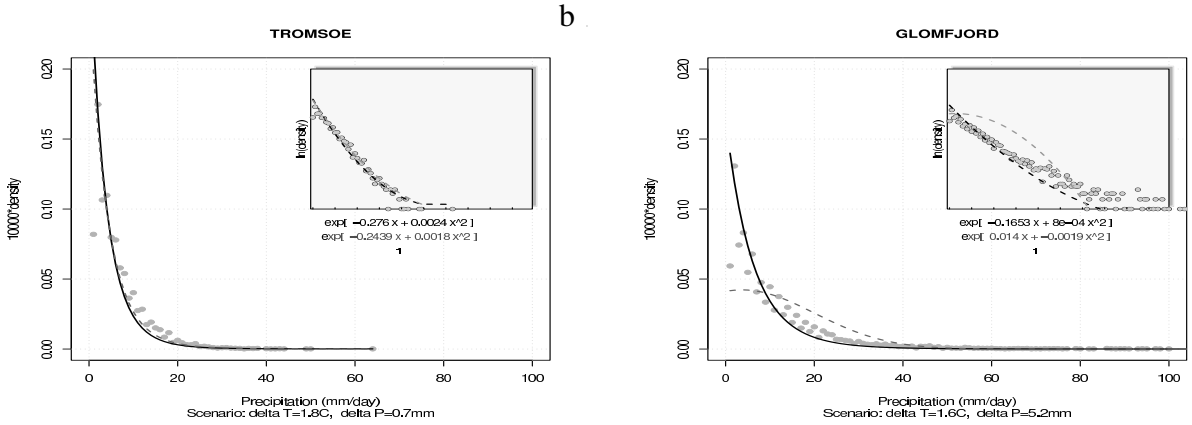

c d

Figure 12: Inter-comparison of results derived for Oslo through various strategies for September–November 2000. Panels a–c show downscaled Gamma parameters based on SLP, temperature and precipitation respectively.

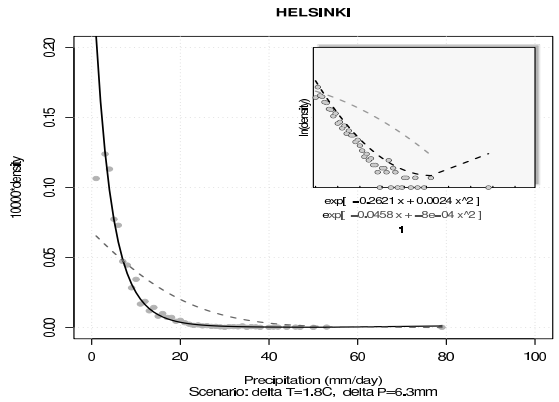

e

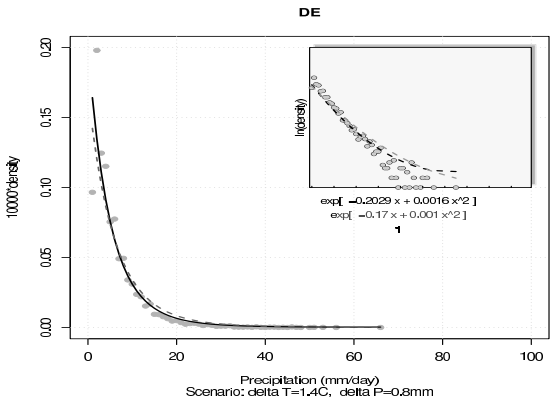

f

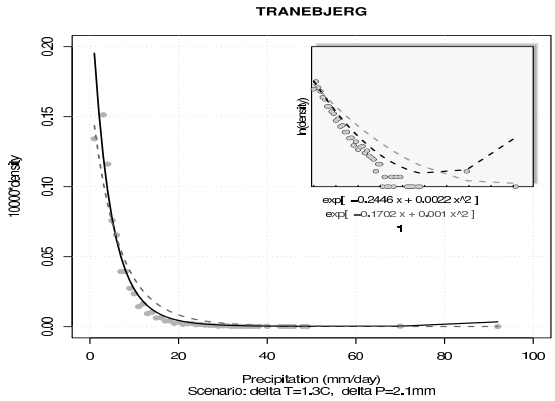

g

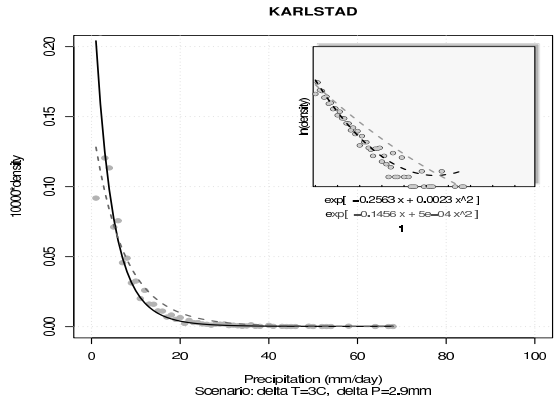

h

Figure 13: Figure 12 continued.

References

Abaurrea, J., & Asín, J., 2005. Forecasting local daily prcipitation patterns in a climate change scenario. *28*.

Benestad, R.E., 2003. How often can we expect a record-event? *Climate Research*, **25**, 3–13.

Benestad, R.E., 2004a. Empirical-Statistical Downscaling in Climate Modeling. *Eos*, **Volume 85**(42), p. 417.

Benestad, R.E., 2004b. Record-values, non-stationarity tests and extreme value distributions. *Global Planetary Change*, **44**(doi:10.1016/j.gloplacha.2004.06.002), 11–26.

Benestad, R.E., 2005. Climate change scenarios for northern Europe from multi-model IPCC AR4 climate simulations. *Geophys. Res. Lett.*, **32**(doi:10.1029/2005GL023401), in press.

Benestad, R.E., & Melsom, A., 2002. Is there a link between the unusually wet autumns in southeastern Norway and SST anomalies? *Climate Research*, **23**(December), 67–79.

Benestad, R.E., Hanssen-Bauer, I., & Førland, E.J., submitted. On Statistical Models for Local Precipitation. *International Journal of Climatology*.

Dehn, M., 1999. Application of an analog downscaling technique to the assessment of future landslide activity - a case study in the Italian Alps. *Climate Research*, **13**, 103–113.

Feddersen, H., & Andersen, U., 2005. A method for statistical downscaling of seasonal ensemble predctions. *Tellus*, **57A**, 398–408.

Fernandez, E., 2005. *On the influence of predictors area in statistical downscaling of daily parameters*. Climate 09/2005. Norwegian Meteorological Institute, www.met.no.

Fernandez, J., & Saenz, J., 2003. Improved field reconstruction with the analog method: searching the CCA space. *Climate Research*, **24**, 199–213.

Feuerstein, B., Dotzek, N., & Grieser, J., 2005. Assessing a Tornado Climatology from Global Tornado Intensity Distributions. *Journal of Climate*, **18**, 585–596.

Grotch, S., & MacCracken, M., 1991. The use of general circulation models to predict regional climate change. *Journal of Climate*, **4**, 286–303.

Hayhoe, K., Cayan, D., Field, C.B., Frumhoff, P.C., Maurer, E.P., Miller, N.L., Moser, S.C., Schneider, S.H., Cahill, K.N., Cleland, E.E., Dale, L., Drapek, R., Hanemann, R.M., Kalkstein, L.S., Lenihan, J., Lunch, C.K., Neilson, R.P., Sheridan, S.C., & Verville, J.H., 2004. Emission pathways, climate change, and impacts on California. *Pages 12422–12427 of: PNAS*, vol. 101. National Academy of Sciences.

Imbert, A., 2003. *The Analog method applied to downscaling of climate scenarios*. KLIMA 08/03. The Norwegian Meteorological Institute, PO Box 43 Blindern, 0313 Oslo, Norway (www.met.no).

Imbert, A., & Benestad, R.E., 2005. An improvement of analog model strategy for more reliable local climate change scenarios. *Theoretical and Applied Climatology*, **82**(DOI: 10.1007/s00704-005-0133-4), 245–255.

Klein Tank, A.M.G.and J. B. Wijngaard, Können, G. P., Böhm, R., Demarée, G., Gocheva, A., Mileta, M., Pashiardis, S., Hejkrlik, L., Kern-Hansen, C., Heino, R., Bessemoulin, P., Müller-Westermeier, G., Tzanakou, M., Szalai, S., Pálsdóttir, T., Fitzgerald, D., Rubin, S., Capaldo, M., Maugeri, M., Leitass, A., Bukantis, A., Aberfeld, R., van Engelen, A. F. V., Førland, E., Mietus, M., Coelho, F., Mares, C., Razuvaev, V., Nieplova, E., Cegnar, T., López, J. Antonio, Dahlström, B., Moberg, A., Kirchhofer, W., Ceylan, A., Pachaliuk, O., Alexander, L. V., & Petrovic, P., 2002. Daily dataset of 20th-century surface air temperature and precipitation series for the European Climate Assessment. *International Journal of Climatology*, **22**, 1441–1453. Data and metadata available at http://eca.knmi.nl.

Pryor, S.C., School, J.T., & Barthelmie, R.J., submitted. Empirical downscaling of wind speed probability distributions. *Journal of Geophysical Research*.

Salathé, E.P., 2005. Downscaling Simulations of Future Global Climate with Application to Hydrologic Modelling. *International Journal of Climatology*, **25**, 419–436.

Schmidli, J., & Frei, C., 2005. Trends of heavy precipitation and wet and dry spells in Switzerland during the 20th Century. *International Journal of Climatology*, **25**(doi: 10.1002/joc.1179), 753–771.

Schoof, J.T., & Pryor, S.C., 2001. Downscaling temperature and precipiation: A comparison of regression-based methods and artificial neural networks. *International Journal of Climatology*, **21**, 773–790.

Simmons, A.J., & Gibson, J.K., 2000. *The ERA-40 Project Plan*. ERA-40 Project Report Series 1. ECMWF, www.ecmwf.int.

Tveito, O.E., & Førland, E.J., 1999. Mapping temperatures in Norway applying terrain information, geostatistics and GIS. *Norsk geografisk tidsskrift*, **53**, 202–212.

van den Dool, H.M., 1995. Constructed Analogue Prediction of the East Central Tropical Pacific through Spring 1996. *NOAA: Experimental Long-Lead Forecast Bulletin*, **4**, 41–43.

von Storch, H., Zorita, E., & Cubasch, U., 1993. Downscaling of Global Climate Change Estimates to Regional Scales: An Application to Iberian Rainfall in Wintertime. *Journal of Climate*, **6**, 1161–1171.

Wilks, D.S., 1995. *Statistical Methods in the Atmospheric Sciences*. Orlando, Florida, USA: Academic Press.

Zorita, E., & von Storch, H., 1999. The Analog Method as a Simple Statistical Downscaling Technique: Comparison with More Complicated Methods. *Journal of Climate*, **12**, 2474–2489.

7 Appendix A

7.1 Derivation of the analytical expression

7.1.1 Analytical expression for the percentile

$$p = 1 - \int_{x=0}^{q_p} -me^{mx}dx = [-e^{mx}]_0^{q_p} = -e^{mq_p} + 1 \quad m < 0 \tag{12}$$

$$\therefore q_p = \frac{\log(1-p)}{m}$$

7.1.2 Analytical expression for relationship between m and $\overline{x_R}$

$$\overline{x_R} = \int_{x=0}^{\infty} -mxe^{mx}dx = -\frac{1}{m} \quad m < 0 \tag{13}$$

8 Appendix B

8.1 Statistics for downscaling of the Gamma parameters

Shape

Conventional:

	Estimate	Std. Error	t value	Pr($>\|t\|$)
(Intercept)	-2.190e-18	2.619e-02	-8.36e-17	1.0000
X1	-1.064e-02	5.809e-03	-1.832	0.0740 .
X2	-1.314e-02	6.451e-03	-2.038	0.0479 *
Transformed:				
(Intercept)	4.136e-18	1.633e-02	2.53e-16	1.0000
X1	-6.614e-03	3.622e-03	-1.826	0.0751 .
X2	-8.382e-03	4.022e-03	-2.084	0.0434 *
X3	-7.848e-03	5.079e-03	-1.545	0.1300

Signif. codes: 0 '***' 0.001 '**' 0.01 '*' 0.05 '.' 0.1 ' ' 1

Conventional: Residual standard error: 0.1757 on 42 degrees of freedom, Multiple R-Squared: 0.1517, Adjusted R-squared: 0.1113, F-statistic: 3.755 on 2 and 42 DF, p-value: 0.03159.

Transformed: Residual standard error: 0.1095 on 41 degrees of freedom, Multiple R-Squared: 0.1964, Adjusted R-squared: 0.1376, F-statistic: 3.341 on 3 and 41 DF, p-value: 0.02835.

Scale

Conventional:

	Estimate	Std. Error	t value	Pr($>\|t\|$)
(Intercept)	-3.837e-17	3.966e-01	-9.67e-17	1
Transformed:				
(Intercept)	2.549e-19	5.226e-03	4.88e-17	1.00
X1	1.891e-03	1.159e-03	1.632	0.11

Conventional: Residual standard error: 2.66 on 44 degrees of freedom. Transformed: Residual standard error: 0.03506 on 43 degrees of freedom, Multiple R-Squared: 0.0583, Adjusted R-squared: 0.0364, F-statistic: 2.662 on 1 and 43 DF, p-value: 0.1101.

Average

	Estimate	Std. Error	t value	Pr($>\|t\|$)
(Intercept)	-1.954e-17	1.958e-01	-9.98e-17	1.00000
X1	-1.254e-01	4.344e-02	-2.886	0.00614 **
X8	-4.021e-01	2.776e-01	-1.448	0.15493

Signif. codes: 0 '***' 0.001 '**' 0.01 '*' 0.05 '.' 0.1 ' ' 1

Residual standard error: 1.314 on 42 degrees of freedom, Multiple R-Squared: 0.1988, Adjusted R-squared: 0.1606, F-statistic: 5.21 on 2 and 42 DF, p-value: 0.009522.

Std

	Estimate	Std. Error	t value	Pr($>\|t\|$)
(Intercept)	-3.735e-17	2.508e-01	-1.49e-16	1.0000
X1	-1.275e-01	5.564e-02	-2.292	0.0269 *

Signif. codes: 0 '***' 0.001 '**' 0.01 '*' 0.05 '.' 0.1 ' ' 1

Residual standard error: 1.683 on 43 degrees of freedom, Multiple R-Squared: 0.1088, Adjusted R-squared: 0.08812, F-statistic: 5.252 on 1 and 43 DF, p-value: 0.02688.